Pergamon

Geochimica et Cosmochimica Acta, Vol. 68, No. 22, pp. 4727-4743, 2004

0016-7037/04 $30.00 + .00

doi:10.1016/j.gca.2004.04.023

Inter-mineral Fe isotope variations in mantle-derived rocks and implications for the Fe geochemical cycle

BRIAN L. BEARD* and CLARK M. JOHNSON

Department of Geology and Geophysics, University of Wisconsin-Madison, 1215 West Dayton Street, Madison, WI 53706, USA

(*Received November* 13, 2003; *accepted in revised form* April 27, 2004)

Abstract—Iron isotope and major- and minor-element compositions of coexisting olivine, clinopyroxene, and orthopyroxene from eight spinel peridotite mantle xenoliths; olivine, magnetite, amphibole, and biotite from four andesitic volcanic rocks; and garnet and clinopyroxene from seven garnet peridotite and eclogites have been measured to evaluate if inter-mineral Fe isotope fractionation occurs in high-temperature igneous and metamorphic minerals and if isotopic fractionation is related to equilibrium Fe isotope partitioning or a result of open-system behavior. There is no measurable fractionation between silicate minerals and magnetite in andesitic volcanic rocks, nor between olivine and orthopyroxene in spinel peridotite mantle xenoliths. There are some inter-mineral differences (up to 0.2‰ in $^{56}Fe/^{54}Fe$) in the Fe isotope composition of coexisting olivine and clinopyroxene in spinel peridotites. The Fe isotope fractionation observed between clinopyroxene and olivine appears to be a result of open-system behavior based on a positive correlation between the $\Delta^{56}Fe_{clinopyroxene\text{-}olivine}$ fractionation and the $\delta^{56}Fe$ value of clinopyroxene and olivine. There is also a significant difference in the isotopic compositions of garnet and clinopyroxene in garnet peridotites and eclogites, where the average $\Delta^{56}Fe_{clinopyroxene\text{-}garnet}$ fractionation is $+0.32 \pm 0.07$‰ for six of the seven samples. The one sample that has a lower $\Delta^{56}Fe_{clinopyroxene\text{-}garnet}$ fractionation of 0.08‰ has a low Ca content in garnet, which may reflect some crystal chemical control on Fe isotope fractionation. The Fe isotope variability in mantle-derived minerals is interpreted to reflect subduction of isotopically variable oceanic crust, followed by transport through metasomatic fluids. Isotopic variability in the mantle might also occur during crystal fractionation of basaltic magmas within the mantle if garnet is a liquidus phase. The isotopic variations in the mantle are apparently homogenized during melting processes, producing homogenous Fe isotope compositions during crust formation.

1. INTRODUCTION

Basaltic, intermediate, and rhyolitic igneous rocks have indistinguishable Fe isotope compositions (Beard et al., 2003a). The constant Fe isotope composition of igneous rocks over a wide range in silica contents (e.g., 45–77 wt.% SiO_2) may be taken as strong evidence that mineral-melt Fe isotope fractionations are small. For example, assuming Rayleigh fractionation of a basaltic melt, if the bulk mineral-melt Fe isotope fractionation was greater than 0.3‰ in $^{56}Fe/^{54}Fe$, intermediate composition magmas produced by fractional crystallization of a basaltic melt (e.g., ~40% crystallization) would produce intermediate composition magmas that had a $\delta^{56}Fe$ value 0.15‰ less than the basaltic magma (Fig. 1). In contrast to the empirical observation that mineral-melt Fe isotope fractionation factors at magmatic temperatures are likely to be small, theoretical and some empirical observations suggest that inter-mineral Fe isotope fractionation factors at temperatures greater than 500°C may be significant (>0.1‰ in $^{56}Fe/^{54}Fe$).

Calculated Fe isotope fractionation factors between clinopyroxene and olivine, or magnetite and olivine at temperatures of 800°C are +0.15 and +0.5‰ in $^{56}Fe/^{54}Fe$, respectively (Polyakov and Mineev, 2000; Fig. 2). Recent reports appear to confirm high-temperature inter-mineral Fe isotope fractionations based on analysis of coexisting olivine, orthopyroxene, and clinopyroxene, as well as magnetite and silicate minerals, in natural samples (Zhu et al., 2002; Berger and von Blanckenburg, 2001; Fig. 2). If significant Fe isotope variations commonly occur in high-temperature environments, the narrow range of Fe isotope compositions measured in igneous rocks remains unexplained.

To evaluate these contradictory observations, here we report the results of a survey of Fe isotope compositions of minerals from high-temperature igneous and metamorphic rocks. The dataset includes Fe isotope analyses of olivine, orthopyroxene, and clinopyroxene from eight spinel peridotites, magnetite and silicate phases (olivine, amphibole, and biotite) from four silicic volcanic rocks, and garnet and pyroxene from seven garnet-bearing metamorphic rocks (garnet peridotites, pyroxenites, and eclogites). The magnitude of the Fe isotope fractionations that have been reported (e.g., Zhu et al., 2002) or calculated (Polyakov and Mineev, 2000) are just analytically resolvable at the 2-σ level (e.g., ±0.14‰, for fractionation between two phases), and we therefore report duplicate or triplicate analyses for nearly every sample to fully document the *external* reproducibility of the dataset. The *accuracy* of the Fe isotope measurements is assessed through Fe isotope analyses of synthetic mineral samples that were prepared from aqueous metal solutions of known Fe isotope compositions. Electron microprobe analyses of the same mineral separates used for Fe isotope analysis are used to constrain equilibrium temperatures, as well as evaluate possible disequilibrium effects.

2. ANALYTICAL METHODS AND NOMENCLATURE

All Fe isotope measurements were conducted using a Micromass IsoProbe, a single-focusing, multi-collector inductively-coupled-plasma

* Author to whom correspondence should be addressed (beardb@geology.wisc.edu).

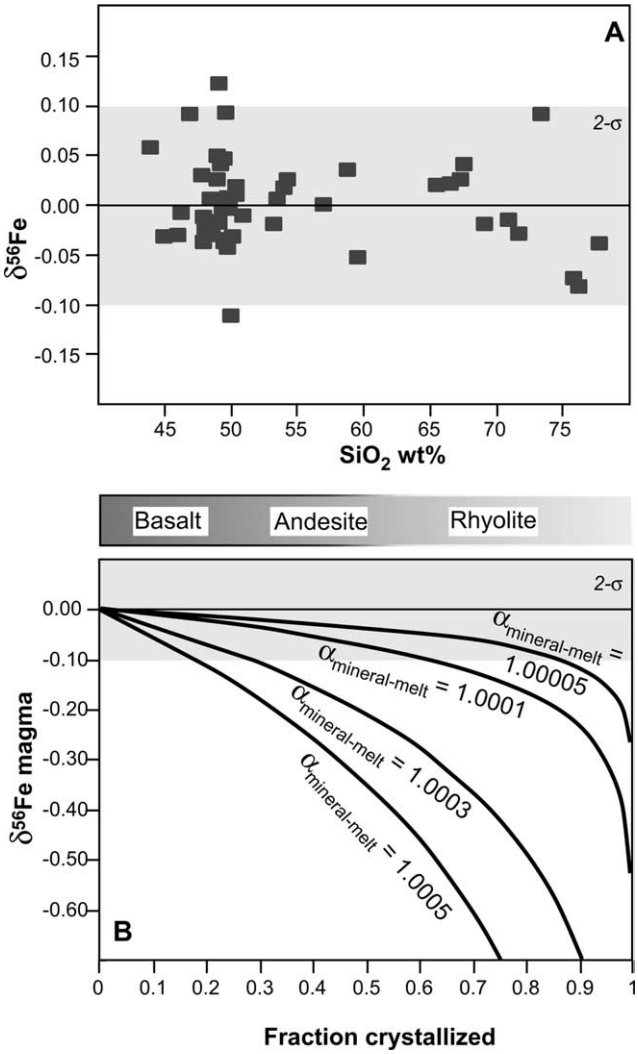

Fig. 1. (A) Plot of Fe isotope composition of igneous rocks measured by Beard et al. (2003a) and this study (average of amphibole and magnetite from Chaos Craig samples) vs. bulk-rock SiO_2 contents measured for the sample or inferred based on similar rock type (e.g., mid-ocean ridge basalt data randomly assigned SiO_2 wt.% between 49 and 50 wt.%; ocean island basalt data inferred based on measured compositions from rocks from the same area). Gray shaded field is two standard deviations of the mean of igneous rocks. (B) Plot of the calculated δ^{56}Fe of a magma vs. percent crystallization assuming different mineral-melt fractionation factors. Rayleigh distillation equation from Taylor and Sheppard (1986); the gray shaded field is two standard deviations of the mean of igneous rocks.

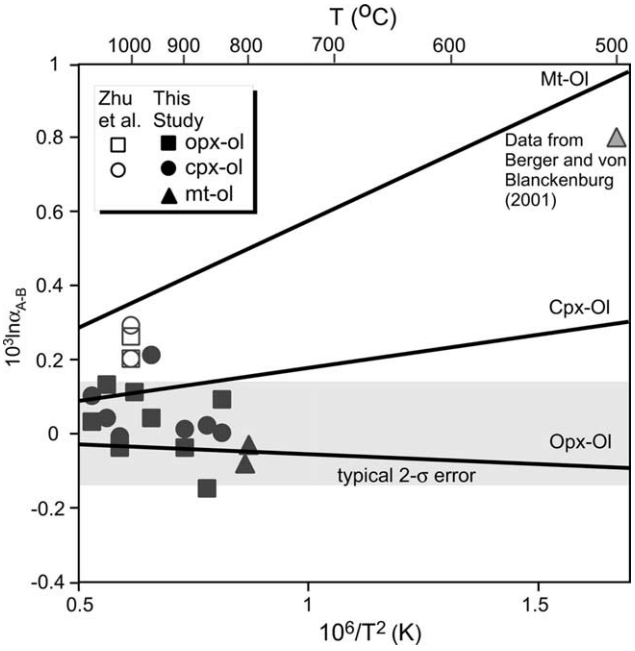

Fig. 2. Plot of $10^3 \ln\alpha_{A\text{-}B}$ values vs. $10^6/T^2$ (T in K) for inter-mineral fractionation between magnetite-olivine, orthopyroxene-olivine, and clinopyroxene-olivine, as calculated from spectroscopic data by Polyakov and Mineev (2000), and as measured from natural samples by Zhu et al. (2002), Berger and von Blanckenburg (2001), and this study. The data from Berger and von Blanckenburg (2001) is the maximum fractionation between magnetite and biotite or chlorite for upper amphibolite and greenschist facies metamorphic rocks.

mass spectrometer with a magnetic-sector mass analyzer. Analyses were conducted on ~400 ppb Fe solutions that were aspirated using a Cetac Aridus desolvating microconcentric nebulizer that was equipped with an all Teflon Elemental Scientific spray chamber and ~50 μL/min self-aspirating nebulizer tip. The methods of Fe isotope analysis and chemical processing of samples followed those reported in Skulan et al. (2002) and Beard et al. (2003a), which consisted of a standard bracketing technique to correct for instrumental mass bias and drift as well as on-peak-zero measurements on blank acid before every isotope ratio measurement. Calculated total analytical blanks based on the measured Fe concentration on the HCl reagent (doubly distilled reagent grade HCl) were less than 1 ng. Each sample passed through columns contained between 50 and 100 μg of Fe, producing a sample to blank ratio >50,000:1. No corrections to isotopic data have been made for blank.

The accuracy and precision of Fe isotope measurements were evaluated using two methods. The precision of Fe isotope analyses was determined by replicating 50 of the 53 samples analyzed in this study. All replicates included processing different aliquots of the sample through ion-exchange columns. The average external 1 standard deviation of these 50 replicate analyses is ± 0.05‰ for δ^{56}Fe and ± 0.07‰ for δ^{57}Fe, which is identical to the external precision obtained by analysis of ultrapure Fe metal standard solutions (Beard et al., 2003a). To test for accuracy of the Fe isotope measurements, synthetic solutions that match the average major-element composition of the sample suite were made using Fe of a known isotopic composition. This approach has been previously used in Fe isotope studies of hydrothermal fluids (Beard et al., 2003b). Twenty-five synthetic solutions were developed that represent six different types of samples prepared using our High Purity Standards (HPS) Fe standard, followed by processing through the entire analytical procedure, and these were analyzed for their Fe isotope compositions (Table 1). The average δ^{56}Fe value of these 25 synthetic solutions is $+0.48 \pm 0.05$‰ (1 SD), which matches the Fe isotope composition of the pure HPS Fe standard (δ^{56}Fe = $+0.49 \pm 0.05$‰; 1 SD, mean of 192 analyses). Using synthetic solutions of known Fe isotope composition that match the chemical matrix of unknown samples is an excellent method for evaluating instrumental mass bias anomalies produced by matrix-induced space charge effects (Albarède and Beard, 2004).

Iron isotope analyses are reported in standard per mil notation using δ^{56}Fe and δ^{57}Fe values, which are defined as:

$$\delta^{56}\mathrm{Fe} = \left(^{56}\mathrm{Fe}/^{54}\mathrm{Fe}_{\mathrm{sample}} / ^{56}\mathrm{Fe}/^{54}\mathrm{Fe}_{\mathrm{standard}} - 1\right) * 10^3, \quad (1)$$

and

$$\delta^{57}\mathrm{Fe} = \left(^{57}\mathrm{Fe}/^{54}\mathrm{Fe}_{\mathrm{sample}} / ^{57}\mathrm{Fe}/^{54}\mathrm{Fe}_{\mathrm{standard}} - 1\right) * 10^3. \quad (2)$$

We use the average of igneous rocks as the standard reference reservoir in calculating δ values (Beard et al., 2003a). Operationally, Fe isotope compositions are determined relative to an ultrapure Fe stan-

Table 1. Fe isotope composition of synthetic samples prepared using HPS Fe.

Sample name	Aliquot	Analysis 1		Analysis 2		Mass spec average		Aliquot average	
		δ^{56}Fe	δ^{57}Fe	δ^{56}Fe	δ^{57}Fe	δ^{56}Fe	δ^{57}Fe	δ^{56}Fe	δ^{57}Fe
Test solution	1	0.46 ± 0.05	0.77 ± 0.03			0.46 ± 0.05	0.77 ± 0.03	0.49 ± 0.06	0.73 ± 0.06
	2	0.52 ± 0.06	0.73 ± 0.03			0.52 ± 0.06	0.73 ± 0.03		
	3	0.46 ± 0.07	0.72 ± 0.03			0.46 ± 0.07	0.72 ± 0.03		
	4	0.50 ± 0.04	0.75 ± 0.03	0.61 ± 0.05	0.88 ± 0.03	0.55 ± 0.07	0.82 ± 0.09		
	5	0.54 ± 0.10	0.68 ± 0.05	0.50 ± 0.06	0.69 ± 0.03	0.52 ± 0.03	0.69 ± 0.01		
	6	0.42 ± 0.10	0.70 ± 0.05	0.42 ± 0.05	0.68 ± 0.05	0.42 ± 0.01	0.69 ± 0.01		
Olivine A	1	0.51 ± 0.05	0.73 ± 0.03	0.47 ± 0.06	0.70 ± 0.04	0.49 ± 0.03	0.72 ± 0.02	0.49 ± 0.03	0.72 ± 0.02
Olivine B	1	0.56 ± 0.05	0.86 ± 0.04	0.53 ± 0.06	0.80 ± 0.04	0.54 ± 0.02	0.83 ± 0.05	0.52 ± 0.04	0.79 ± 0.07
Olivine B	2	0.49 ± 0.07	0.72 ± 0.05			0.49 ± 0.07	0.72 ± 0.05		
Opx A	1	0.56 ± 0.06	0.78 ± 0.03	0.44 ± 0.06	0.72 ± 0.05	0.50 ± 0.08	0.75 ± 0.05	0.50 ± 0.07	0.75 ± 0.06
Opx A	2	0.55 ± 0.05	0.78 ± 0.03	0.44 ± 0.05	0.68 ± 0.04	0.49 ± 0.08	0.74 ± 0.08		
Opx B	1	0.46 ± 0.06	0.69 ± 0.04	0.48 ± 0.05	0.73 ± 0.03	0.47 ± 0.01	0.71 ± 0.03	0.52 ± 0.04	0.79 ± 0.07
Opx B	2	0.49 ± 0.07	0.72 ± 0.05			0.47 ± 0.09	0.78 ± 0.04		
Cpx A	1	0.50 ± 0.05	0.73 ± 0.03	0.53 ± 0.04	0.76 ± 0.04	0.51 ± 0.02	0.75 ± 0.05	0.48 ± 0.05	0.74 ± 0.03
Cpx A	2	0.50 ± 0.10	0.76 ± 0.04	0.41 ± 0.05	0.71 ± 0.04	0.46 ± 0.06	0.74 ± 0.04		
Cpx B	1	0.41 ± 0.07	0.63 ± 0.04			0.41 ± 0.07	0.63 ± 0.04	0.47 ± 0.06	0.74 ± 0.11
Cpx B	2	0.49 ± 0.05	0.76 ± 0.03			0.49 ± 0.05	0.76 ± 0.03		
Cpx B	3	0.52 ± 0.07	0.85 ± 0.03			0.52 ± 0.07	0.85 ± 0.03		
Omphacite	1	0.37 ± 0.07	0.65 ± 0.04	0.40 ± 0.06	0.64 ± 0.04	0.39 ± 0.02	0.64 ± 0.01	0.46 ± 0.06	0.74 ± 0.12
Omphacite	2	0.50 ± 0.06	0.63 ± 0.03	0.45 ± 0.06	0.75 ± 0.04	0.48 ± 0.03	0.69 ± 0.09		
Omphacite	3	0.50 ± 0.05	0.89 ± 0.02	0.53 ± 0.03	0.88 ± .02	0.51 ± 0.03	0.89 ± 0.01		
Garnet A	1	0.39 ± 0.07	0.66 ± 0.03	0.45 ± 0.06	0.67 ± 0.04	0.42 ± 0.04	0.66 ± 0.01	0.44 ± 0.05	0.67 ± 0.02
Garnet A	2	0.41 ± 0.09	0.66 ± 0.05	0.51 ± 0.06	0.69 ± 0.04	0.46 ± 0.07	0.67 ± 0.02		
Garnet B	1	0.40 ± 0.08	0.63 ± 0.04	0.44 ± 0.06	0.65 ± 0.04	0.42 ± 0.03	0.64 ± 0.02	0.49 ± 0.09	0.76 ± 0.14
Garnet B	2	0.55 ± 0.06	0.92 ± 0.04	0.59 ± 0.08	0.84 ± 0.04	0.57 ± 0.03	0.88 ± 0.06		

Chemical composition of synthetic samples: Test solution: 100.9 ppm Fe, 75.9 ppm Mg, 75.6 ppm Ca, 2.0 ppm Cr, 40.2 ppm Na. Olivine A: 99.4 ppm Fe, 325 ppm Si, 505.0 ppm Mg. Olivine B: 99.6 ppm Fe, 333.5 ppm Si, 505.8 ppm Mg. Opx A: 98.8 ppm Fe, 451.3 ppm Si, 20.1 ppm Al, 347.2 ppm Mg, 6.7 ppm Ca. Opx B: 98.5 ppm Fe, 657.4 ppm Si, 29 ppm Al, 508.4 ppm Mg, 9.6 ppm Ca. Cpx A: 98.6 ppm Fe; 437.4 ppm Si, 15.4 ppm Al, 176.0 ppm Mg, 276.3 ppm Ca. Cpx B: 103 ppm Fe, 2023 ppm Si, 71.8 ppm Al, 827.9 ppm Mg, 1310.9 ppm Ca. Omphacite: 98.5 ppm Fe; 711.5 ppm Si, 131.3 ppm Al, 175.9 ppm Mg, 307.7 ppm Ca, 1.2 ppm Cr, 0.4 ppm Mn, 103.2 ppm Na, 3.3 ppm Ti. Garnet A: 97.9 ppm Fe, 222.7 ppm Sr, 140.9 ppm Al, 103.0 ppm Mg, 86.5 ppm Ca, 0.4 ppm Cr, 2.0 ppm Mn, 0.8 ppm Ti. Garnet B: 98.7 ppm Fe, 289.9 ppm Si, 174.8 ppm Al, 181.8 ppm Mg, 49.1 ppm Ca, 15.3 ppm Cr, 3.6 ppm Ca.

Analysis 1 and 2 refer to different mass spectrometry runs of a sample conducted on different days; the errors are 2 SE from in-run statistics. Mass spec average is the average of up to 2 analyses, the error is 1 standard deviation external, or if there is only 1 mass spectrometry analysis, the error is 2 SE of the in-run statistics. Aliquot average of Replicate is the average of processing different aliquots of a sample throughout the entire analytical procedure, and is probably the best estimate of external reproducibility. The δ^{56}Fe value of the pure HPS Fe standard is +0.49 ± 0.05‰ (1 SD, n = 192).

dard purchased from High Purity Standards (HPS Fe) during mass analysis; this standard is well known relative to igneous rocks using the dataset of Beard et al. (2003a) where the HPS Fe solution has a δ^{56}Fe value of +0.49‰ and a δ^{57}Fe of value of +0.73‰ relative to igneous rocks. From 2001 to 2004, the Fe isotope composition measured for our HPS Fe standard is δ^{56}Fe = +0.49 ± 0.05‰ and δ^{57}Fe = +0.73 ± 0.07‰ (1 SD, n = 192). For a different in-house standard (J-M Fe), the measured Fe isotope composition is δ^{56}Fe = +0.25 ± 0.05‰ and δ^{57}Fe = +0.39 ± 0.08‰ (1 SD; n = 286), and for the certified reference material IRMM-014 (Taylor et al., 1992, 1993) the δ^{56}Fe = −0.09 ± 0.05‰ and δ^{57}Fe = −0.12 ± 0.07‰ (1 SD; n = 263). Interlaboratory comparison of Fe isotope ratios can be made by comparison to the measured Fe isotope composition of the IRMM-014 Fe standard, as discussed in Beard and Johnson (2004).

Iron isotope fractionation between two phases, A and B, is noted as:

$$\alpha_{A-B} = (^{56}Fe/^{54}Fe)_A/(^{56}Fe/^{54}Fe)_B \quad (3)$$

or by the approximation:

$$10^3 \ln\alpha_{A-B} \approx \Delta^{56}Fe_{A-B} = \delta^{56}Fe_A - \delta^{56}Fe_B \quad (4)$$

3. SAMPLE SUITE

Three broad groups of samples have been investigated to evaluate the degree of inter-mineral Fe isotope fractionation at high temperature. Isotope fractionation among olivine, orthopyroxene, and clinopyroxene is determined using spinel peridotites. Zhu et al. (2002) suggested that there are Fe isotope fractionations of +0.2‰ in ^{56}Fe/^{54}Fe ratios, which are significant, at high temperature (900°C) between orthopyroxene and olivine, as well as clinopyroxene and olivine. Similarly, Polyakov and Mineev (2000) calculate a +0.10‰ fractionation in ^{56}Fe/^{54}Fe at 900°C between clinopyroxene and olivine, but an insignificant fractionation (−0.03‰ in ^{56}Fe/^{54}Fe) between orthopyroxene and olivine (Fig. 2). A second group of samples includes mafic enclaves and their host lavas from the Chaos Crags of Mount Lassen, California, and these are used to characterize inter-mineral fractionation between magnetite and the silicate minerals olivine, amphibole, and biotite. These samples allow us to test the predicted fractionation, for example, of −0.5‰ in ^{56}Fe/^{54}Fe between olivine and magnetite at a temperature of 800°C (Polyakov and Mineev, 2000). Moreover, Berger and von Blanckenburg (2001) report a −0.8‰ fractionation in ^{56}Fe/^{54}Fe between biotite and magnetite from samples that formed at high temperature (Fig. 2). A final group of samples, which includes Alpine-type eclogites, garnet peridotites, and garnet pyroxenites, is used to determine the Fe isotope fractionation between garnet and clinopyroxene over a range of mineral compositions and modes.

3.1. Coexisting Olivine-Orthopyroxene-Clinopyroxene

Olivine, orthopyroxene, and clinopyroxene mineral separates were prepared from eight spinel peridotite mantle xenoliths. Three of the samples are from Kilbourne Hole, New Mexico (Bussod and Williams,

Table 2. Major element mineral compositions of spinel peridotites.

Sample	SiO_2	TiO_2	Al_2O_3	Cr_2O_3	FeO	MnO	MgO	CaO	NiO	Na_2O	Sum
Olivine											
H299-15	40.82	na	na	na	9.28	0.14	50.15	0.04	0.36	na	100.78
H30-82-1	40.64	na	na	na	7.61	0.12	51.44	0.03	0.39	na	100.23
OW-3	40.06	na	na	na	9.50	0.15	49.38	0.12	0.32	na	99.51
Ba-4-21	41.07	na	na	na	10.31	0.14	49.27	0.06	0.37	na	101.23
Ba-4-14	40.98	na	na	na	9.71	0.17	49.55	0.05	0.38	na	100.83
KH-8	40.26	na	na	na	9.72	0.15	49.75	0.10	0.42	na	100.40
KH-6	40.66	na	na	na	8.48	0.14	50.90	0.09	0.41	na	100.67
KH-13	40.31	na	na	na	8.00	0.13	50.89	0.16	0.37	na	99.86
Orthopyroxene											
H299-15	55.65	0.06	3.27	0.28	5.70	0.17	34.25	0.44	na	0.06	99.88
H30-82-1	56.58	0.03	1.82	0.75	5.04	0.13	35.73	0.49	na	0.02	100.59
OW-3	53.13	0.15	5.20	0.41	6.04	0.16	32.51	0.91	na	0.12	98.64
Ba-4-21	54.57	0.11	4.67	0.33	6.82	0.14	32.56	0.85	na	0.09	100.14
Ba-4-14	54.91	0.11	4.21	0.38	6.18	0.14	33.35	0.64	na	0.09	100.02
KH-8	53.90	0.11	4.43	0.64	6.76	0.15	32.19	1.20	na	0.14	99.53
KH-6	55.82	0.04	2.60	0.70	5.32	0.12	34.43	0.96	na	0.02	100.00
KH-13	55.82	0.04	2.38	0.90	4.96	0.12	34.01	1.64	na	0.04	99.92
Clinopyroxene											
H299-15	52.66	0.27	4.72	0.65	2.12	0.09	16.11	21.37	na	1.17	99.17
H30-82-1	54.05	0.05	1.77	0.79	1.57	0.08	17.72	23.22	na	0.50	99.74
OW-3	51.10	0.53	7.09	0.74	3.26	0.08	15.71	18.66	na	1.62	98.79
Ba-4-21	51.46	0.48	6.88	0.72	3.36	0.11	15.20	20.03	na	1.57	99.81
Ba-4-14	51.23	0.48	6.68	0.84	2.57	0.10	15.14	20.56	na	1.69	99.30
KH-8	51.61	0.30	5.91	1.29	3.45	0.11	16.35	18.70	na	1.33	99.04
KH-6	53.00	0.06	2.98	1.16	2.39	0.08	17.66	21.45	na	0.51	99.29

na = not analyzed. Oxides are in weight percent. Chemical compositions determined by electron microprobe analysis of grain mounts prepared from the mineral separates that were used for Fe isotope analyses. Compositions are averages determined by 3 electron microprobe spot analyses on two or more mineral grains. All analyses were made by wavelength-dispersive spectrometry using natural minerals as standards with ZAF corrections.

1991), one sample is from the Old Woman Springs, California (Neville et al., 1983; Wilshire et al., 1988), two samples are from Hill 1933, California (Wilshire et al., 1988), and two samples are from Harrat al Kishb, Saudi Arabia (McGuire, 1988; McGuire and Bohannon, 1989). Mineral separates were prepared by coarsely crushing a portion of the xenolith with an agate mortar and pestle and then handpicking optically pure grains using a binocular microscope. Olivine compositions range from Fo_{92} to Fo_{89}, orthopyroxene compositions range from En_{92} to En_{88}, and clinopyroxene compositions range from Di_{86} to $Di_{65,}$ as determined by electron microprobe analysis of grain mounts prepared from the same aliquot of minerals used for Fe isotope analysis (Table 2). Pyroxene endmember compositions were calculated according to Beard et al. (1992). Equilibration temperatures were calculated using the Taylor (1998) calibration of the two-pyroxene geothermometer at an assumed pressure of 15 kilobars. Equilibration temperatures and average Fe isotope compositions are reported in Table 3, and Table 4 reports all duplicate Fe isotope measurements of the mantle xenoliths. Our calculated two-pyroxene equilibration temperatures agree well with the more thorough work of Neville et al. (1983), McGuire (1988), McGuire and Bohannon (1989), and Bussod and Williams (1991) for these xenolith localities. These more extensive geothermometry studies highlight that equilibration temperatures determined by pyroxene solvus thermometry, Fe-Mg exchange between olivine and spinel, as well as Al content in clinopyroxene or orthopyroxene that coexist with olivine and spinel, tend to yield convergent results to within 50°C.

3.2. Coexisting Magnetite-Silicate

Separates of magnetite and amphibole from four samples from the Chaos Crags of Mount Lassen, California were analyzed for their Fe isotope composition (Table 5). Additionally, two of the samples contained olivine and two other samples contained biotite, and these phases were analyzed for their Fe isotope compositions (Table 5). Average mineral compositions determined by electron microprobe are reported in Table 6, and brief petrographic descriptions are reported in Table 5. Equilibration temperatures determined by magnetite-ilmenite thermometry for these four samples ranged from 790 to 805°C (Bradshaw, 2002; Table 3), which are in excellent agreement with previous geothermometry studies conducted on Chaos Crags volcanic rocks by Heiken and Eichelberger (1980).

3.3. Coexisting Garnet-Clinopyroxene

Coexisting garnet and clinopyroxene from seven samples and whole-rock powders from four of these samples were analyzed for their Fe isotope compositions (Table 7). Two samples are garnet peridotites from the Bohemian Massif of the Czech Republic, one is from the Mohelno locality, and the other is from Nove Dvory (Medaris et al., 1990). A garnet pyroxenite vein from the Nove Dvory peridotite body was also analyzed for its Fe isotope composition (Medaris et al., 1995a). Garnet and omphacite from four eclogites were analyzed for their Fe isotope compositions; one sample is from the Alpe Arami peridotite locality in the Swiss Alps (Ernst, 1977), and three samples are Variscan-age eclogites from the Moldanubian zone of the Bohemian Massif in the Czech Republic (Medaris et al., 1995a, 1995b). Temperatures were calculated using Fe-Mg exchange thermometry between garnet and clinopyroxene using major-element compositions determined by electron microprobe on grain mounts made from the same mineral separates that were used for Fe isotope analysis (Table 8). Equilibration temperatures vary between 700 and 1115°C at an assumed pressure of 30 kbars, using the Ellis and Green (1979) calibration (Table 3). These temperatures are consistent with those obtained by more detailed studies conducted on samples from these localities by Medaris et al. (1990, 1995b) and Ernst (1977).

4. RESULTS

The $\delta^{56}Fe$ values of the high-temperature minerals analyzed in this study span a range of nearly 1‰, from $\delta^{56}Fe = -0.5$ to $+0.3$‰. Significant inter-mineral fractionations ($\Delta^{56}Fe_{A\text{-}B}$) exist in a number of samples that exceed the 2-sigma analytical

Table 3. Average Fe isotope composition of minerals from mantle xenoliths, igneous rocks, and garnet-bearing metamorphic rocks and their temperatures of equilibration.

Sample	Rock type	Equil. temp.	δ^{56}Fe Ol	δ^{56}Fe Opx	δ^{56}Fe Cpx	δ^{56}Fe Mt	δ^{56}Fe Amp	δ^{56}Fe Bt	δ^{56}Fe Gt	$\Delta^{56}Fe_{Opx\text{-}Ol}$	$\Delta^{56}Fe_{Cpx\text{-}Ol}$	$\Delta^{56}Fe_{Ol\text{-}Mt}$	$\Delta^{56}Fe_{Amp\text{-}Mt}$	$\Delta^{56}Fe_{Bt\text{-}Mt}$	$\Delta^{56}Fe_{Cpx\text{-}Gt}$
H2991-5	Sp Pd	894[a]	−0.01 ± 0.08	−0.05 ± 0.08	0.00 ± 0.06	na	na	na	na	−0.04 ± 0.11	0.01 ± 0.10	nd	nd	nd	nd
H30-82-1	Sp Pd	835[a]	−0.12 ± 0.06	−0.03 ± 0.03	−0.12 ± 0.03	na	na	na	na	0.09 ± 0.06	0.00 ± 0.06	nd	nd	nd	nd
OW-3	Sp Pd	1058[a]	−0.22 ± 0.01	−0.09 ± 0.04	−0.18 ± 0.08	na	na	na	na	0.13 ± 0.04	0.04 ± 0.08	nd	nd	nd	nd
Ba-4-21	Sp Pd	960[a]	−0.52 ± 0.06	−0.48 ± 0.07	−0.31 ± 0.04	na	na	na	na	0.04 ± 0.09	0.21 ± 0.08	nd	nd	nd	nd
Ba-4-14	Sp Pd	858[a]	−0.02 ± 0.06	−0.17 ± 0.09	0.00 ± 0.02	na	na	na	na	−0.15 ± 0.10	0.02 ± 0.06	nd	nd	nd	nd
KH-8	Sp Pd	1100[a]	−0.34 ± 0.04	−0.31 ± 0.04	−0.24 ± 0.05	na	na	na	na	0.03 ± 0.06	0.10 ± 0.07	nd	nd	nd	nd
KH-6	Sp Pd	1027[a]	−0.02 ± 0.07	−0.06 ± 0.08	−0.03 ± 0.05	na	na	na	na	−0.04 ± 0.10	−0.01 ± 0.09	nd	nd	nd	nd
KH-13	Sp Pd	1000[b]	−0.17 ± 0.05	−0.06 ± 0.04	—	na	na	na	na	0.11 ± 0.06	nd	nd	nd	nd	nd
00LH7	B. And	804[c]	−0.07 ± 0.07	na	na	0.01 ± 0.08	−0.05 ± 0.15	na	na	nd	nd	0.08 ± 0.11	−0.04 ± 0.17	nd	nd
98LH8	B. And	800[d]	−0.01 ± 0.04	na	na	0.02 ± 0.04	−0.01 ± 0.07	na	na	nd	nd	0.03 ± 0.06	−0.03 ± 0.08	nd	nd
00LH6	Dacite	798[c]	na	na	na	0.03 ± 0.04	0.05 ± 0.05	−0.08 ± 0.03	na	nd	nd	nd	0.02 ± 0.06	−0.11 ± 0.05	nd
98LH7	Dacite	794[c]	na	na	na	0.07 ± 0.08	−0.02 ± 0.04	0.05 ± 0.01	na	nd	nd	nd	−0.09 ± 0.09	−0.02 ± 0.08	nd
CS-MH-2	Gt Pd	1110[e]	—	—	0.07 ± 0.06	na	na	na	−0.17 ± 0.07	nd	nd	nd	nd	nd	0.24 ± 0.09
CS-ND-2A	Gt Pd	699[e]	—	—	0.00 ± 0.05	na	na	na	−0.39 ± 0.04	nd	nd	nd	nd	nd	0.39 ± 0.07
CS-ND-3B	Gt Px	958[e]	na	na	−0.03 ± 0.05	na	na	na	−0.10 ± 0.04	nd	nd	nd	nd	nd	0.07 ± 0.06
AA-4	Eclo	835[e]	na	na	0.30 ± 0.07	na	na	na	0.01 ± 0.12	nd	nd	nd	nd	nd	0.29 ± 0.14
CS-UR-1	Eclo	1115[e]	na	na	0.15 ± 0.04	na	na	na	−0.16 ± 0.03	nd	nd	nd	nd	nd	0.31 ± 0.05
CS-BN-4	Eclo	816[e]	na	na	0.22 ± 0.06	na	na	na	−0.20 ± 0.01	nd	nd	nd	nd	nd	0.42 ± 0.06
CS-BK-2	Eclo	812[e]	na	na	0.26 ± 0.06	na	na	na	−0.01 ± 0.04	nd	nd	nd	nd	nd	0.27 ± 0.07

na = phase does not occur in sample; — = phase not analyzed but is present in sample; nd = not determined.

"a" Equilibration temperatures determined for "a" using the Taylor (1998) calibration of the two-pyroxene geothermometer at an assumed pressure of 15 kbars using the mineral compositions reported in Table 2; for "b" temperature inferred from other samples from the Kilbourne Hole xenolith locality; for "c" temperatures are based on coexisting ilmentie and magnetite pairs determined by Bradshaw (2002); for "d" temperature inferred from other samples from the same locality; for "e" temperatures determined using the Ellis and Green (1979) calibration of the garnet clinopyroxene Fe-Mg exchange thermometer at an assumed pressure of 30 kbars.

Iron isotope data summarized in Tables 4, 5, and 7.

Rock types: Sp Pd = spinel peridotite; B. And = basaltic andesite; Dacite = rhyodacite; Gt Pd = garnet peridotite; Gt Px = garnet pyroxenite; Eclo = eclogite.

Table 4. Fe isotope composition of olivine, clinopyroxene, and orthopyroxene from mantle xenoliths.

Sample name	Mineral	Aliquot	Note	Analysis 1		Analysis 2		Analysis 3		Mass spec average		Aliquot average	
				δ^{56}Fe	δ^{57}Fe	δ^{56}Fe	δ^{57}Fe	δ^{56}Fe	δ^{57}Fe	δ^{56}Fe	δ^{57}Fe	δ^{56}Fe	δ^{57}Fe
KH-6	Olivine	1	1	0.04 ± 0.08	0.04 ± 0.04	−0.13 ± 0.06	−0.09 ± 0.03			−0.04 ± 0.12	−0.02 ± 0.09	−0.02 ± 0.07	0.00 ± 0.08
KH-6	Olivine	2	1	0.03 ± 0.06	0.10 ± 0.03					0.03 ± 0.06	0.10 ± 0.03		
KH-6	Olivine	3	1	−0.05 ± 0.10	0.00 ± 0.04	0.00 ± 0.06	−0.07 ± 0.03			−0.02 ± 0.03	−0.04 ± 0.04		
KH-6	Cpx	1	1	0.06 ± 0.07	0.19 ± 0.05	−0.07 ± 0.07	−0.04 ± 0.03			0.00 ± 0.09	0.07 ± 0.17	−0.03 ± 0.05	0.03 ± 0.10
KH-6	Cpx	2	1	−0.07 ± 0.07	−0.04 ± 0.03					−0.07 ± 0.07	−0.04 ± 0.03		
KH-6	Cpx	3	1	−0.04 ± 0.09	0.01 ± 0.04	−0.06 ± 0.07	0.02 ± 0.04			−0.05 ± 0.01	0.02 ± 0.01		
KH-6	Opx	1	1	−0.08 ± 0.07	−0.06 ± 0.03	−0.15 ± 0.06	−0.12 ± 0.04			−0.11 ± 0.05	−0.09 ± 0.05	−0.06 ± 0.08	−0.07 ± 0.04
KH-6	Opx	2	1	−0.04 ± 0.05	−0.03 ± 0.03					−0.04 ± 0.05	−0.03 ± 0.03		
KH-6	Opx	3	1	0.03 ± 0.08	−0.06 ± 0.04					0.03 ± 0.08	−0.06 ± 0.04		
KH-8	Olivine	1	1	−0.30 ± 0.07	−0.43 ± 0.04					−0.30 ± 0.07	−0.43 ± 0.04	−0.34 ± 0.04	−0.44 ± 0.07
KH-8	Olivine	2	1	−0.31 ± 0.05	−0.36 ± 0.03	−0.34 ± 0.05	−0.41 ± 0.03			−0.32 ± 0.02	−0.38 ± 0.04		
KH-8	Olivine	3	1	−0.34 ± 0.07	−0.45 ± 0.04	−0.41 ± 0.05	−0.54 ± 0.03			−0.37 ± 0.05	−0.50 ± 0.06		
KH-8	Cpx	1	1	−0.22 ± 0.05	−0.29 ± 0.04					−0.22 ± 0.05	−0.29 ± 0.04	−0.24 ± 0.05	−0.31 ± 0.02
KH-8	Cpx	2	1	−0.30 ± 0.06	−0.31 ± 0.03	−0.28 ± 0.06	−0.34 ± 0.04			−0.29 ± 0.01	−0.33 ± 0.02		
KH-8	Cpx	3	1	−0.19 ± 0.10	−0.29 ± 0.04					−0.19 ± 0.10	−0.29 ± 0.04		
KH-8	Opx	1	1	−0.26 ± 0.07	−0.37 ± 0.04					−0.26 ± 0.07	−0.37 ± 0.04	−0.31 ± 0.04	−0.40 ± 0.03
KH-8	Opx	2	1	−0.36 ± 0.05	−0.44 ± 0.03	−0.33 ± 0.05	−0.42 ± 0.03			−0.34 ± 0.02	−0.43 ± 0.01		
KH-8	Opx	3	1	−0.31 ± 0.11	−0.38 ± 0.05					−0.31 ± 0.11	−0.38 ± 0.05		
KH-13	Olivine	1	1	−0.12 ± 0.05	−0.19 ± 0.03					−0.12 ± 0.05	−0.19 ± 0.03	−0.17 ± 0.05	−0.23 ± 0.03
KH-13	Olivine	2	1	−0.22 ± 0.02	−0.27 ± 0.03	−0.20 ± 0.06	−0.24 ± 0.03	−0.13 ± 0.06	−0.21 ± 0.03	−0.18 ± 0.05	−0.24 ± 0.03		
KH-13	Olivine	A	1	−0.16 ± 0.09	−0.29 ± 0.04					−0.16 ± 0.09	−0.29 ± 0.04	−0.16 ± 0.09	−0.29 ± 0.04
KH-13	Opx	1	1	−0.03 ± 0.06	0.01 ± 0.03	−0.11 ± 0.04	−0.08 ± 0.03			−0.07 ± 0.05	−0.04 ± 0.06	−0.06 ± 0.04	−0.01 ± 0.06
KH-13	Opx	2	1	−0.05 ± 0.07	0.03 ± 0.04					−0.05 ± 0.07	0.03 ± 0.04		
OW-3	Olivine	1	2	−0.21 ± 0.07	−0.33 ± 0.04					−0.21 ± 0.07	−0.33 ± 0.04	−0.22 ± 0.01	−0.32 ± 0.02
OW-3	Olivine	2	2	−0.22 ± 0.07	−0.30 ± 0.04					−0.22 ± 0.07	−0.30 ± 0.04		
OW-3	Olivine	3	2	−0.21 ± 0.09	−0.34 ± 0.03					−0.21 ± 0.09	−0.34 ± 0.03		
OW-3	Cpx	1	2	−0.16 ± 0.06	−0.21 ± 0.03					−0.16 ± 0.06	−0.21 ± 0.03	−0.18 ± 0.08	−0.25 ± 0.07
OW-3	Cpx	2	2	−0.29 ± 0.05	−0.34 ± 0.03	−0.11 ± 0.06	−0.18 ± 0.04			−0.20 ± 0.12	−0.26 ± 0.12		
OW-3	Cpx	3	2	−0.16 ± 0.08	−0.26 ± 0.04					−0.16 ± 0.08	−0.26 ± 0.04		
OW-3	Opx	1	2	−0.05 ± 0.07	−0.15 ± 0.04					−0.05 ± 0.07	−0.15 ± 0.04	−0.09 ± 0.04	−0.15 ± 0.06
OW-3	Opx	2	2	−0.10 ± 0.05	−0.18 ± 0.03					−0.10 ± 0.05	−0.18 ± 0.03		
OW-3	Opx	3	2	−0.14 ± 0.08	−0.09 ± 0.04	−0.08 ± 0.07	−0.06 ± 0.04			−0.11 ± 0.04	−0.07 ± 0.01		
Ba-4-21	Olivine	1	3	−0.51 ± 0.07	−0.76 ± 0.03					−0.51 ± 0.07	−0.76 ± 0.03	−0.52 ± 0.01	−0.76 ± 0.02
Ba-4-21	Olivine	2	3	−0.52 ± 0.06	−0.74 ± 0.04	−0.52 ± 0.09	−0.77 ± 0.05			−0.52 ± 0.01	−0.76 ± 0.02		
Ba-4-21	Olivine	A	3	−0.40 ± 0.05	−0.70 ± 0.03	−0.61 ± 0.06	−0.77 ± 0.04	−0.52 ± 0.06	−0.76 ± 0.03	−0.51 ± 0.10	−0.74 ± 0.04	−0.52 ± 0.08	−0.75 ± 0.03
Ba-4-21	Olivine	B	3	−0.58 ± 0.05	−0.77 ± 0.03	−0.49 ± 0.07	−0.75 ± 0.05			−0.54 ± 0.06	−0.76 ± 0.02		
Ba-4-21	Cpx	1	3	−0.28 ± 0.05	−0.43 ± 0.03					−0.28 ± 0.05	−0.43 ± 0.03	−0.31 ± 0.04	−0.48 ± 0.06
Ba-4-21	Cpx	2	3	−0.35 ± 0.03	−0.54 ± 0.03	−0.30 ± 0.06	−0.47 ± 0.03			−0.33 ± 0.04	−0.51 ± 0.06		
Ba-4-21	Opx	1	3	−0.49 ± 0.06	−0.67 ± 0.03					−0.49 ± 0.06	−0.67 ± 0.03	−0.48 ± 0.07	−0.69 ± 0.06
Ba-4-21	Opx	2	3	−0.41 ± 0.05	−0.65 ± 0.03	−0.54 ± 0.06	−0.76 ± 0.03			−0.48 ± 0.10	−0.71 ± 0.08		
Ba-4-14	Olivine	1	3	0.03 ± 0.05	−0.10 ± 0.04	−0.03 ± 0.06	−0.07 ± 0.04	−0.14 ± 0.05	−0.23 ± 0.03	−0.04 ± 0.08	−0.13 ± 0.08	−0.04 ± 0.07	−0.10 ± 0.09
Ba-4-14	Olivine	2	3	−0.02 ± 0.05	−0.01 ± 0.03					−0.02 ± 0.05	−0.01 ± 0.03		
Ba-4-14	Olivine	A	3	0.00 ± 0.06	0.15 ± 0.04					0.00 ± 0.06	0.15 ± 0.04	0.00 ± 0.01	0.07 ± 0.11
Ba-4-14	Olivine	B	3	0.01 ± 0.05	0.00 ± 0.02					0.01 ± 0.05	0.00 ± 0.03		
Ba-4-14	Cpx	1	3	−0.01 ± 0.07	0.12 ± 0.03					−0.01 ± 0.07	0.12 ± 0.03	0.00 ± 0.02	0.06 ± 0.09
Ba-4-14	Cpx	2	3	0.01 ± 0.06	0.00 ± 0.03					0.01 ± 0.06	0.00 ± 0.03		
Ba-4-14	Opx	1	3	−0.07 ± 0.06	0.05 ± 0.03	−0.22 ± 0.09	−0.19 ± 0.05			−0.14 ± 0.11	−0.07 ± 0.17	−0.17 ± 0.09	−0.12 ± 0.15
Ba-4-14	Opx	2	3	−0.22 ± 0.07	−0.24 ± 0.04					−0.22 ± 0.07	−0.24 ± 0.04		
H30-82-1	Olivine	1	4	−0.08 ± 0.08	0.06 ± 0.04					−0.08 ± 0.08	−0.06 ± 0.04	−0.12 ± 0.06	−0.12 ± 0.16
H30-82-1	Olivine	2	4	−0.09 ± 0.06	−0.20 ± 0.04	−0.18 ± 0.07	−0.22 ± 0.03			−0.14 ± 0.06	−0.21 ± 0.02		

Table 4. (Continued).

Sample name	Mineral	Aliquot	Note	Analysis 1		Analysis 2		Analysis 3		Mass spec average		Aliquot average	
				δ^{56}Fe	δ^{57}Fe	δ^{56}Fe	δ^{57}Fe	δ^{56}Fe	δ^{57}Fe	δ^{56}Fe	δ^{57}Fe	δ^{56}Fe	δ^{57}Fe
H30-82-1	Cpx	1	4	−0.15 ± 0.06	−0.20 ± 0.05					−0.15 ± 0.06	−0.20 ± 0.05	−0.12 ± 0.03	−0.18 ± 0.06
H30-82-1	Cpx	2	4	−0.12 ± 0.06	−0.23 ± 0.03	−0.09 ± 0.05	−0.11 ± 0.03			−0.10 ± 0.02	−0.17 ± 0.09		
H30-82-1	Opx	1	4	−0.06 ± 0.05	−0.07 ± 0.03					−0.06 ± 0.05	−0.07 ± 0.03	−0.03 ± 0.03	−0.03 ± 0.04
H30-82-1	Opx	2	4	−0.01 ± 0.05	−0.03 ± 0.03	−0.02 ± 0.05	0.01 ± 0.03			−0.01 ± 0.01	−0.01 ± 0.03		
H299-15	Olivine	1	4	−0.06 ± 0.06	−0.11 ± 0.04					−0.06 ± 0.06	−0.11 ± 0.04	−0.01 ± 0.08	−0.04 ± 0.10
H299-15	Olivine	2	4	0.05 ± 0.06	0.04 ± 0.03					0.05 ± 0.06	0.04 ± 0.03		
H299-15	Cpx	1	4	−0.05 ± 0.09	−0.03 ± 0.04	0.09 ± 0.06	0.11 ± 0.03			0.02 ± 0.10	0.04 ± 0.10	0.00 ± 0.06	0.03 ± 0.08
H299-15	Cpx	2	4	−0.01 ± 0.06	0.09 ± 0.04	−0.02 ± 0.07	−0.04 ± 0.04			−0.02 ± 0.01	0.02 ± 0.10		
H299-15	Opx	1	4	−0.10 ± 0.05	−0.02 ± 0.03	0.08 ± 0.07	−0.02 ± 0.04	−0.04 ± 0.08	−0.01 ± 0.04	−0.02 ± 0.09	−0.02 ± 0.01	−0.05 ± 0.08	−0.03 ± 0.03
H299-15	Opx	2	4	−0.09 ± 0.07	−0.03 ± 0.03	−0.12 ± 0.06	−0.09 ± 0.04			−0.11 ± 0.07	−0.06 ± 0.03		

Notes: 1: Spinel peridotite mantle xenolith from Kilbourne Hole, New Mexico; 2: Spinel peridotite mantle xenolith from Old Woman Springs, locality 22 of Wilshire et al., 1988; 3: Spinel peridotite mantle xenolith from Hill 1933, California; locality 35 of Wilshire et al., 1988; 4: Spinel peridotite mantle xenolith from Harrat al Kishb, Saudi Arabia (McGuire and Bohannon, 1989).

Analysis 1, 2, and 3 refer to different mass spectrometry runs of a sample conducted on different days; the errors are 2 SE from in-run statistics. Mass spec average is the average of up to 3 analyses, the error is 1 standard deviation external, or if there is only 1 mass spectrometry analysis, the error is 2 SE of the in-run statistics. Aliquot average is the average of processing different aliquots of a sample throughout the entire analytical procedure, and is probably the best estimate of external reproducibility. Aliquots 1, 2, and 3 are replicates of the same mineral dissolution, and aliquots A and B are replicate analyses of a different mineral separate prepared from the sample.

errors, which is estimated to be ±0.14‰ for $\Delta^{56}Fe_{A\text{-}B}$, based on the square root of the sum of the squares for the error in the individual δ values, where their 2σ error is ±0.1‰

4.1. Olivine-Orthopyroxene-Clinopyroxene Fractionations

The Fe isotope compositions of olivine, clinopyroxene, and orthopyroxene from the spinel peridotite mantle xenoliths are variable, and δ^{56}Fe values range from −0.52 to 0.00‰ (Table 4). On "δ-δ" plots of δ^{56}Fe of olivine relative to that of orthopyroxene or clinopyroxene (Fig. 3A and 3B, respectively), the δ^{56}Fe values of the phases are positively correlated. Orthopyroxene-olivine fractionations ($\Delta^{56}Fe_{opx\text{-}ol}$) range from −0.15 to +0.13‰, but there is no correlation between δ^{56}Fe of olivine or orthopyroxene and $\Delta^{56}Fe_{opx\text{-}ol}$ values. Clinopyroxene-olivine fractionations ($\Delta^{56}Fe_{cpx\text{-}ol}$) range from −0.01 to +0.21‰, and in this case, $\Delta^{56}Fe_{cpx\text{-}ol}$ increases as the δ^{56}Fe value of clinopyroxene or olivine decreases. Correlations between mineral chemistry and Fe isotope composition are difficult to evaluate because of the relatively small range in isotopic and chemical compositions and the fact that only eight samples have been analyzed. However, those samples that have the largest $\Delta^{56}Fe_{cpx\text{-}ol}$ values correspond to samples which have the lowest olivine forsterite contents (molar Mg/(Mg+Fe) ratio; Fig. 3C) and molar Mg/(Fe+Mg) clinopyroxene ratios (not shown). Additionally, olivine, orthopyroxene, and clinopyroxene that have the most negative δ^{56}Fe values have high Fe contents and Fe/Mg ratios (Fig. 4).

4.2. Magnetite-Silicate Fractionations

Magnetite, amphibole, olivine, and biotite from the Chaos Crag volcanic rocks have δ^{56}Fe values that range from −0.08 to +0.07‰ (Table 5). Based on these samples, there appear to be no resolvable inter-mineral Fe isotope fractionations between silicate minerals and magnetite; $\Delta^{56}Fe_{olivine\text{-}magnetite}$ is 0.08 and 0.03‰, $\Delta^{56}Fe_{biotite\text{-}magnetite}$ is −0.11 and −0.02‰, and $\Delta^{56}Fe_{amphibole\text{-}magnetite}$ is −0.09 to 0.02‰, for the pairs studied (Table 3; Fig. 5). Because these samples are rapidly quenched volcanic rocks, it seems likely that the near-zero fractionations between silicates and magnetite reflect equilibrium conditions.

4.3. Garnet-Clinopyroxene Fractionations

Garnets and clinopyroxene from garnet peridotites, pyroxenites, and eclogites have δ^{56}Fe values that range from −0.39 to +0.01‰, and −0.03 to +0.30‰, respectively (Table 7). The Fe isotope compositions of coexisting garnet and clinopyroxene are positively correlated (Fig. 6A), and six of the seven samples have $\Delta^{56}Fe_{cpx\text{-}gt}$ of ~+0.3‰, whereas one sample (CS-ND-3B) has a significantly lower $\Delta^{56}Fe_{cpx\text{-}gt}$ fractionation of 0.07‰. Mass-balance calculations using the measured Fe contents and isotope compositions, as well as visually estimated modal proportions of garnet and clinopyroxene, indicate that the bulk Fe in these peridotites, pyroxenite, and eclogites should have δ^{56}Fe values between −0.10 to +0.07‰, which overlap those measured in the bulk-rock samples (Table 7). In the case of eclogites, this observation is consistent with the homogeneous Fe isotope composition measured in bulk-rock basalts (Beard et al., 2003a). Excluding sample CS-ND-3B,

Table 5. Fe isotope composition of magnetite, amphibole, olivine, and biotite of igneous rocks from Lassen Volcanic National Park.

Sample name	Mineral	Aliquot	Note	Analysis 1		Analysis 2		Analysis 3		Mass spec average		Aliquot average	
				δ^{56}Fe	δ^{57}Fe	δ^{56}Fe	δ^{57}Fe	δ^{56}Fe	δ^{57}Fe	δ^{56}Fe	δ^{57}Fe	δ^{56}Fe	δ^{57}Fe
98LH8	Mt	1	1	−0.03 ± 0.06	0.02 ± 0.03					−0.03 ± 0.06	0.02 ± 0.03	0.02 ± 0.04	0.04 ± 0.03
98LH8	Mt	2	1	0.03 ± 0.06	0.01 ± 0.03					0.03 ± 0.06	0.01 ± 0.03		
98LH8	Mt	3	1	0.07 ± 0.06	0.07 ± 0.04	0.02 ± 0.07	0.07 ± 0.03			0.04 ± 0.04	0.07 ± 0.01		
98LH8	Ol	1	1	0.02 ± 0.05	0.02 ± 0.03					0.02 ± 0.05	0.02 ± 0.03	−0.01 ± 0.04	0.00 ± 0.03
98LH8	Ol	2	1	−0.04 ± 0.07	−0.02 ± 0.04					−0.04 ± 0.07	−0.02 ± 0.04		
98LH8	Amph	1	1	−0.07 ± 0.08	−0.08 ± 0.03	−0.02 ± 0.06	−0.01 ± 0.03			−0.04 ± 0.04	−0.04 ± 0.04	−0.01 ± 0.07	0.02 ± 0.09
98LH8	Amph	2	1	0.08 ± 0.04	0.13 ± 0.03	−0.05 ± 0.06	0.05 ± 0.04			0.01 ± 0.10	0.09 ± 0.04		
00LH7	Mt	1	2	0.07 ± 0.07	0.08 ± 0.04					0.07 ± 0.07	0.08 ± 0.04	0.01 ± 0.08	0.04 ± 0.06
00LH7	Mt	2	2	−0.05 ± 0.07	−0.01 ± 0.05					−0.05 ± 0.07	−0.01 ± 0.05		
00LH7	Ol	1	2	−0.02 ± 0.06	−0.09 ± 0.04					−0.02 ± 0.06	−0.09 ± 0.04	−0.07 ± 0.07	−0.14 ± 0.03
00LH7	Ol	2	2	−0.01 ± 0.05	−0.14 ± 0.03	−0.13 ± 0.06	−0.17 ± 0.04			−0.07 ± 0.08	−0.15 ± 0.02		
00LH7	Ol	3	2	−0.13 ± 0.08	−0.15 ± 0.04					−0.13 ± 0.08	−0.15 ± 0.04		
00LH7	Amph	1	2	0.11 ± 0.08	0.15 ± 0.04	−0.04 ± 0.06	0.05 ± 0.04			0.03 ± 0.08	0.10 ± 0.04	−0.05 ± 0.15	−0.07 ± 0.22
00LH7	Amph	2	2	−0.26 ± 0.04	−0.38 ± 0.04	−0.10 ± 0.05	−0.21 ± 0.03	0.07 ± 0.09	0.04 ± 0.06	−0.10 ± 0.17	−0.19 ± 0.21		
00LH6	Mt	1	3	0.06 ± 0.06	0.19 ± 0.03					0.06 ± 0.06	0.19 ± 0.03	0.03 ± 0.04	0.13 ± 0.07
00LH6	Mt	2	3	0.00 ± 0.05	0.08 ± 0.03					0.00 ± 0.05	0.08 ± 0.03		
00LH6	Biotite	1	3	−0.10 ± 0.06	−0.17 ± 0.04					−0.10 ± 0.06	−0.17 ± 0.04	−0.08 ± 0.03	−0.06 ± 0.15
00LH6	Biotite	2	3	−0.05 ± 0.06	0.04 ± 0.04					−0.05 ± 0.06	0.04 ± 0.04		
00LH6	Amph	1	3	0.05 ± 0.05	0.07 ± 0.04					0.05 ± 0.05	0.07 ± 0.04	0.05 ± 0.05	0.07 ± 0.04
98LH7	Mt	1	4	0.18 ± 0.06	0.17 ± 0.04	0.05 ± 0.05	0.15 ± 0.04			0.12 ± 0.09	0.16 ± 0.01	0.07 ± 0.08	0.11 ± 0.07
98LH7	Mt	2	4	0.08 ± 0.05	0.13 ± 0.03	−0.05 ± 0.06	0.05 ± 0.04			0.01 ± 0.10	0.09 ± 0.06		
98LH7	Biotite	1	4	0.05 ± 0.06	−0.02 ± 0.03					0.05 ± 0.06	−0.02 ± 0.03	0.05 ± 0.01	0.03 ± 0.07
98LH7	Biotite	2	4	0.04 ± 0.07	0.08 ± 0.04					0.04 ± 0.07	0.08 ± 0.04		
98LH7	Amph	1	4	0.01 ± 0.06	0.05 ± 0.04					0.01 ± 0.06	0.05 ± 0.04	−0.02 ± 0.04	0.02 ± 0.05
98LH7	Amph	2	4	−0.05 ± 0.06	−0.02 ± 0.04					−0.05 ± 0.06	−0.02 ± 0.04		

Notes: 1: Basaltic andesite inclusion in rhyodacite host from dome B of Chaos Crags, Lassen Volcanic National Park, California; 2: Basaltic andesite inclusion in rhyodacite host from dome F of Chaos Crags, Lassen Volcanic National Park, California; 3: Rhyodacite from dome F of Chaos Crags, Lassen Volcanic National Park, California; 4: Rhyodacite from dome B of Chaos Crags, Lassen Volcanic National Park, California.

Analysis 1, 2, and 3 refer to different mass spectrometry runs of a sample conducted on different days; the errors are 2 SE from in-run statistics. Mass spec average is the average of up to 3 analyses, the error is 1 standard deviation external, or if there is only 1 mass spectrometry analysis, the error is 2 SE of the in-run statistics. Aliquot average is the average of processing different aliquots of a sample throughout the entire analytical procedure, and is probably the best estimate of external reproducibility. Aliquots 1, 2, and 3 are replicates of the same mineral dissolution.

Table 6. Major element mineral compositions of magnetite-bearing igneous rocks.

Sample	SiO_2	TiO_2	Al_2O_3	Cr_2O_3	Fe_2O_3[a]	FeO	MnO	MgO	CaO	NiO	Na_2O	K_2O	Sum
Magnetite													
2000LH7	na	5.51	1.83	0.04	54.26	33.32	0.64	0.94	na	na	na	na	96.54
1998LH8	na	5.33	1.50	0.04	54.94	33.29	0.64	0.81	na	na	na	na	96.55
2000LH6	na	4.72	1.40	0.04	56.55	32.35	0.63	1.09	na	na	na	na	65.77
1998LH7	na	4.79	1.47	0.08	56.41	32.42	0.75	1.07	na	na	na	na	96.98
Amphibole													
2000LH7	41.25	2.16	11.84	0.01	—	11.38	0.17	14.55	11.00	na	2.15	0.28	94.97
1998LH8	41.08	1.97	11.86	0.02	—	11.88	0.23	13.75	10.82	na	2.14	0.23	93.98
2000LH6	48.97	1.05	5.15	0.01	—	11.70	0.66	15.55	11.03	na	1.02	0.37	95.51
1998LH7	48.52	0.99	5.24	0.01	—	11.43	0.59	15.58	11.20	na	1.08	0.33	94.97
Olivine													
2000LH7	38.54	na	na	na	—	17.13	0.25	42.80	0.14	0.07	na	na	98.93
1998LH8	39.73	na	na	na	—	17.30	0.28	43.08	0.13	0.08	na	na	100.59
Biotite													
2000LH6	36.31	4.11	13.10	0.01	—	14.78	0.19	14.79	0.02	na	0.78	7.88	91.97
1998LH7	36.42	4.15	12.99	0.01	—	14.44	0.22	14.76	0.04	na	0.77	7.98	91.77

na = not analyzed. Oxides are in weight percent.

[a] Magnetite Fe_2O_3 contents were calculated by charge balance, Fe_2O_3 contents for other minerals were not calculated. Chemical compositions determined by electron microprobe analysis of grain mounts prepared from the mineral separates that were used for Fe isotope analyses. Compositions are averages determined by 3 electron microprobe spot analyses on two or more mineral grains. All analyses were made by wavelength-dispersive spectrometry using natural minerals as standards with ZAF corrections.

samples which have the smallest $\Delta^{56}Fe_{cpx\text{-}gt}$ fractionations have higher Fe-Mg equilibration temperatures as compared to samples with larger $\Delta^{56}Fe_{cpx\text{-}gt}$ fractionations (Fig. 6). There are no clear correlations between mineral composition and Fe isotope composition; however, the sample with the smallest $\Delta^{56}Fe_{cpx\text{-}gt}$ fractionation does have the lowest grossular content in garnet (Fig. 6C).

5. DISCUSSION

Our results indicate that there is no measurable difference in Fe isotope compositions among Fe-bearing minerals that are common liquidus phases in crustal magmas, including olivine, amphibole, and biotite. Moreover, the $\delta^{56}Fe$ values of magnetite and coexisting silicate minerals in volcanic rocks are the same as those measured for terrestrial igneous rocks (Beard et al., 2003a). These observations stand in marked contrast to the calculated $\Delta^{56}Fe_{olivine\text{-}magnetite}$ fractionation of $-0.5‰$ at 800°C, using the fractionation factors of Polyakov and Mineev (2000). The magnetite-silicate fractionations measured in this study are not consistent with the inter-mineral Fe isotope variations reported by Berger and von Blanckenburg (2001) between magnetite and other silicate minerals measured in high-temperature metamorphic rocks. The reason for the differences between this study and that conducted by Berger and von Blanckenburg (2001) is unknown. Some of the discrepancy may lie in the nature of the samples; those analyzed in this study are quickly cooled volcanic rocks, whereas the greenschist- and amphibolite-grade metamorphic rocks analyzed by Berger and von Blanckenburg (2001) cooled much more slowly. It is possible, therefore, that open-system isotopic exchange between magnetite and silicates during slow cooling of the metamorphic rocks produced a larger apparent isotopic fractionation. Similar differences in inter-mineral fractionations for slowly cooled metamorphic rocks as compared to rapidly quenched volcanic rocks have been documented for O isotope fractionation between silicates and magnetite (Chiba et al., 1989)

There are significant differences in Fe isotope compositions between garnet and clinopyroxene in eclogites and garnet-bearing ultramafic rocks, where $\Delta^{56}Fe_{cpx\text{-}garnet}$ fractionations range from $+0.42$ to $+0.07‰$. We interpret these fractionations to reflect equilibrium partitioning given the fact that six of the seven garnet-clinopyroxene pairs scatter about a $\Delta^{56}Fe_{cpx\text{-}garnet}$ value of $+0.30‰$, over a $0.4‰$ range in $\delta^{56}Fe$ values for the individual minerals (Fig. 6A). The one sample (CS-ND-3B) that has a low $\Delta^{56}Fe_{cpx\text{-}gt}$ fractionation of $+0.07‰$, and does not follow the same trend as the others, has a very low garnet Ca content (Fig. 6C), and it remains to be seen if Ca content in garnet plays the same crystal chemical control on Fe isotope fractionation as it does for O isotope fractionation (Kohn and Valley, 1998; Valley et al., 2003). Significant Fe isotope fractionation between garnet and clinopyroxene raises the possibility that Fe isotope variations may be produced within the mantle during crystal fractionation of basalts at mantle pressures, where garnet may be a liquidus phase.

For eclogites where the bulk of the Fe budget in the rock is from garnet, the $\delta^{56}Fe$ value of garnet is close to zero. In contrast, the $\delta^{56}Fe$ value of garnet in peridotite is high, and this reflects the fact that only a small fraction of the total rock Fe inventory is contained in garnet; the phase(s) which contains the major portion of Fe in the total rock is clinopyroxene (and presumably olivine and orthopyroxene), which has a $\delta^{56}Fe$ value close to zero and equal to that measured for the bulk rock. Olivine and orthopyroxene were not analyzed from these massif-type peridotites because these minerals have been extensively serpentinized during retrograde metamorphism. These internally consistent mass-balance relations confirm the accuracy of the $\delta^{56}Fe$ values determined on the minerals, and support our earlier conclusion that the $\delta^{56}Fe$ value of bulk igneous rocks is very homogenous.

Table 7. Fe isotope composition of garnet and clinopyroxene from massif-type eclogites and garnet peridotites.

Sample name	Mineral	Aliquot	Note	Analysis 1		Analysis 2		Mass spec average		Aliquot average	
				δ^{56}Fe	δ^{57}Fe	δ^{56}Fe	δ^{57}Fe	δ^{56}Fe	δ^{57}Fe	δ^{56}Fe	δ^{57}Fe
CS-MH-2	Garnet	1	1	−0.19 ± 0.05	−0.19 ± 0.03	−0.12 ± 0.05	−0.16 ± 0.03	−0.15 ± 0.05	−0.18 ± 0.02	−0.17 ± 0.07	−0.18 ± 0.05
CS-MH-2	Garnet	2	1	−0.26 ± 0.05	−0.24 ± 0.03	−0.12 ± 0.06	−0.11 ± 0.03	−0.19 ± 0.10	−0.17 ± 0.09		
CS-MH-2	Cpx	1	1	0.01 ± 0.05	0.06 ± 0.04	0.09 ± 0.05	0.21 ± 0.03	0.05 ± 0.06	0.14 ± 0.10		
CS-MH-2	Cpx	A	1	0.11 ± 0.06	0.13 ± 0.04			0.11 ± 0.06	0.13 ± 0.04		
CS-MH-2	WR	1	1	−0.03 ± 0.07	−0.06 ± 0.04	−0.07 ± 0.07	−0.13 ± 0.04	−0.03 ± 0.00	−0.12 ± 0.08	−0.02 ± 0.04	−0.09 ± 0.07
CS-MH-2	WR	2	1	−0.07 ± 0.07	−0.13 ± 0.04	0.04 ± 0.07	0.01 ± 0.04	−0.02 ± 0.08	−0.06 ± 0.10		
CS-MH-2	WR	3	1	−0.03 ± 0.07	−0.07 ± 0.04			−0.03 ± 0.07	−0.07 ± 0.04		
CS-ND-2A	Garnet	1	2	−0.42 ± 0.04	−0.67 ± 0.03	−0.36 ± 0.06	−0.52 ± 0.03	−0.39 ± 0.04	−0.59 ± 0.10		
CS-ND-2A	Cpx	1	2	−0.03 ± 0.06	−0.05 ± 0.03	−0.02 ± 0.05	0.05 ± 0.03	−0.03 ± 0.01	0.00 ± 0.07		
CS-ND-2A	Cpx	A	2	0.06 ± 0.05	−0.02 ± 0.03			0.06 ± 0.05	−0.02 ± 0.03		
CS-ND-3B	Garnet	1	3	−0.15 ± 0.08	−0.17 ± 0.03			−0.15 ± 0.08	−0.17 ± 0.03	−0.10 ± 0.04	−0.16 ± 0.02
CS-ND-3B	Garnet	2	3	−0.08 ± 0.06	−0.13 ± 0.03	−0.08 ± 0.05	−0.17 ± 0.03	−0.08 ± 0.00	−0.15 ± 0.02		
CS-ND-3B	Cpx	1	3	−0.02 ± 0.06	0.10 ± 0.04			−0.02 ± 0.06	0.10 ± 0.04		
CS-ND-3B	Cpx	A	3	−0.08 ± 0.05	−0.05 ± 0.04	0.02 ± 0.06	0.00 ± 0.03	−0.03 ± 0.07	−0.03 ± 0.04		
CS-UR-1	Garnet	1	4	−0.14 ± 0.07	−0.23 ± 0.04			−0.14 ± 0.07	−0.23 ± 0.03	−0.16 ± 0.03	−0.26 ± 0.06
CS-UR-1	Garnet	2	4	−0.20 ± 0.07	−0.33 ± 0.04	−0.15 ± 0.05	−0.22 ± 0.03	−0.17 ± 0.04	−0.28 ± 0.08		
CS-UR-1	Cpx	1	4	0.19 ± 0.07	0.25 ± 0.04			0.19 ± 0.07	0.25 ± 0.04		
CS-UR-1	Cpx	A	4	0.16 ± 0.05	0.19 ± 0.03	0.12 ± 0.06	0.27 ± 0.03	0.14 ± 0.03	0.23 ± 0.06		
CS-UR-1	WR	1	4	−0.09 ± 0.06	−0.13 ± 0.04			−0.09 ± 0.06	−0.13 ± 0.04	−0.06 ± 0.03	−0.07 ± 0.06
CS-UR-1	WR	2	4	−0.05 ± 0.07	−0.07 ± 0.04			−0.05 ± 0.07	−0.07 ± 0.04		
CS-UR-1	WR	3	4	−0.03 ± 0.05	−0.02 ± 0.03			−0.03 ± 0.05	−0.02 ± 0.03		
CS-BN-4	Garnet	1	5	−0.19 ± 0.06	−0.25 ± 0.04	−0.20 ± 0.04	−0.28 ± 0.03	−0.20 ± 0.01	−0.26 ± 0.02		
CS-BN-4	Cpx	1	5	0.15 ± 0.06	0.29 ± 0.04			0.15 ± 0.06	0.29 ± 0.04	0.22 ± 0.06	0.34 ± 0.04
CS-BN-4	Cpx	2	5	0.25 ± 0.06	0.37 ± 0.04	0.26 ± 0.05	0.35 ± 0.03	0.25 ± 0.01	0.36 ± 0.02		
CS-BN-4	WR	1	5	−0.06 ± 0.07	−0.13 ± 0.04			−0.06 ± 0.07	−0.13 ± 0.04	−0.03 ± 0.05	−0.06 ± 0.07
CS-BN-4	WR	2	5	0.03 ± 0.06	0.03 ± 0.03	−0.08 ± 0.07	−0.11 ± 0.04	−0.03 ± 0.08	−0.04 ± 0.10		
CS-BN-4	WR	3	5	−0.02 ± 0.04	−0.03 ± 0.03			−0.02 ± 0.04	−0.03 ± 0.03		
CS-BK-2	Garnet	1	6	0.04 ± 0.08	−0.09 ± 0.03			0.04 ± 0.08	−0.09 ± 0.03	−0.01 ± 0.04	−0.02 ± 0.10
CS-BK-2	Garnet	2	6	−0.03 ± 0.06	0.10 ± 0.05	−0.02 ± 0.06	−0.08 ± 0.03	−0.03 ± 0.01	0.01 ± 0.12		
CS-BK-2	Cpx	1	6	0.20 ± 0.09	0.39 ± 0.05			0.20 ± 0.09	0.39 ± 0.05	0.26 ± 0.06	0.43 ± 0.04
CS-BK-2	Cpx	2	6	0.27 ± 0.05	0.44 ± 0.03	0.32 ± 0.04	0.46 ± 0.03	0.30 ± 0.04	0.45 ± 0.02		
AA-4	Garnet	1	7	0.14 ± 0.06	0.21 ± 0.04	0.08 ± 0.11	0.19 ± 0.07	0.11 ± 0.06	0.20 ± 0.04	0.01 ± 0.12	0.07 ± 0.16
AA-4	Garnet	2	7	−0.13 ± 0.04	−0.10 ± 0.03	−0.03 ± 0.08	−0.03 ± 0.05	−0.08 ± 0.04	−0.06 ± 0.03		
AA-4	Cpx	1	7	0.37 ± 0.08	0.57 ± 0.04			0.37 ± 0.08	0.57 ± 0.04		
AA-4	Cpx	A	7	0.23 ± 0.06	0.25 ± 0.03	0.30 ± 0.05	0.44 ± 0.03	0.27 ± 0.05	0.35 ± 0.13		
AA-4	WR	1	7	0.05 ± 0.06	0.08 ± 0.03			0.05 ± 0.06	0.08 ± 0.03	−0.02 ± 0.06	0.01 ± 0.08
AA-4	WR	2	7	−0.04 ± 0.07	−0.01 ± 0.03	−0.09 ± 0.05	−0.09 ± 0.03	−0.07 ± 0.04	−0.05 ± 0.03		
AA-4	WR	3	7	−0.01 ± 0.06	0.07 ± 0.03			−0.01 ± 0.06	0.07 ± 0.03		

Notes: 1: Garnet peridotite from Mohelno, Czech Republic (Medaris et al., 1990); 2: Garnet peridotite from Nove Dvory, Czech Republic (Medaris et al., 1990); 3: Garnet pyroxenite vein from Nove Dvory, Czech Rebupulic (Medaris et al., 1995a); 4: Eclogite Uhrov, Czech Republic (Medaris et al., 1995a, 1995b); 5: Eclogite Bernatice, Czech Republic (Medaris et al., 1995b); 6: Eclogite Borek, Czech Republic (Medaris et al., 1995b); 7: Eclogite Alpe Arami, Switzerland (Ernst, 1977).

Analysis 1 and 2 refer to different mass spectrometry runs of a sample conducted on different days; the errors are 2 SE from in-run statistics. Mass spec average is the average of up to 3 analyses, the error is 1 standard deviation external, or if there is only 1 mass spectrometry analysis, the error is 2 SE of in-run statistics. Aliquot average is the average of processing different aliquots of a sample throughout the entire analytical procedure, which is probably the best estimate of external reproducibility. Aliquots 1, 2, and 3 are replicates of the same mineral or whole-rock dissolution, and aliquot A is a replicate analyses of a different mineral separate prepared from the sample.

Table 8. Major element mineral compositions of eclogites, garnet peridotites, and garnet pyroxenite.

Sample	SiO_2	TiO_2	Al_2O_3	Cr_2O_3	FeO	MnO	MgO	CaO	Na_2O	Sum
Garnet										
AA-4	39.87	0.04	21.46	0.03	18.32	0.40	8.40	10.62	na	99.16
CS-UR-1	40.76	0.09	21.52	0.12	12.26	0.36	11.00	13.08	na	99.19
CS-BN-4	39.61	0.03	21.17	0.07	20.81	0.44	7.75	9.55	na	99.42
CS-BK-2	38.86	0.09	20.78	0.01	23.38	0.63	4.86	10.83	na	99.44
CS-ND-2A	39.99	0.04	21.51	0.04	18.30	0.37	8.30	11.07	na	99.63
CS-ND-3B	41.87	0.16	21.95	0.68	9.00	0.31	18.41	6.31	na	98.68
CS-MH-2	41.94	0.18	22.03	0.62	8.58	0.28	17.72	7.41	na	98.75
Clinopyroxene										
AA-4	55.64	0.13	11.97	0.08	2.78	0.04	8.80	13.87	6.52	99.81
CS-UR-1	55.62	0.12	11.87	0.03	2.73	0.04	8.81	13.85	6.48	99.55
CS-BN-4	54.77	0.11	7.45	0.05	4.36	0.05	11.02	17.14	4.63	99.58
CS-BK-2	54.31	0.14	9.23	0.02	5.58	0.04	8.95	14.85	5.67	98.81
CS-ND2A	4.81	0.20	2.77	1.17	2.84	0.10	15.72	20.03	2.33	99.97
CS-ND-3B	54.68	0.20	2.82	0.10	2.33	0.04	16.29	21.89	1.44	99.79
CS-MH-2	52.31	0.58	6.75	1.13	2.85	0.11	15.23	19.47	1.86	100.30

na = not analyzed. Oxides are in weight percent. Chemical compositions determined by electron microprobe analysis of grain mounts prepared from the mineral separates that were used for Fe isotope analyses. Compositions are averages determined by 3 electron microprobe spot analyses on two or more mineral grains. All analyses were made by wavelength-dispersive spectrometry using natural minerals as standards with ZAF corrections.

The inter-mineral Fe isotope fractionations measured for the eight analyzed spinel peridotites are variable. There is no apparent inter-mineral Fe isotope fractionation between olivine and orthopyroxene, where $\Delta^{56}Fe_{opx\text{-}ol}$ fractionations vary from +0.12 to −0.14‰, and do not correlate with $\delta^{56}Fe$ values. For comparison, the calculated Fe isotope fractionation between orthopyroxene and olivine is −0.03‰ at 1000°C, using the fractionation factors of Polyakov and Mineev (2000), consistent with the lack of a measurable Fe isotope fractionation between orthopyroxene and olivine in this study. In contrast, the Fe isotope data presented by Zhu et al. (2002) for two spinel peridotite xenoliths yield $\Delta^{56}Fe_{opx\text{-}ol}$ fractionations of +0.20 and +0.26‰ (Fig. 3A). The xenoliths analyzed by Zhu et al. (2002) equilibrated at similar temperatures as the xenoliths from this study; therefore the differences in inter-mineral Fe isotope fractionation measured here relative to Zhu et al. (2002) cannot be a result of simple temperature dependence of the $\Delta^{56}Fe_{opx\text{-}ol}$ fractionation factor.

Using the fractionation factors of Polyakov and Mineev (2000), the predicted $\Delta^{56}Fe_{cpx\text{-}ol}$ fractionation is +0.09‰ at 1000°C. Three clinopyroxene-olivine pairs that Zhu et al. (2002) analyzed have $\Delta^{56}Fe_{cpx\text{-}ol}$ fractionations that range from +0.12 to +0.29‰ at equilibration temperatures between 900 and 1000 °C. The clinopyroxene-olivine pairs analyzed in this study have $\Delta^{56}Fe_{cpx\text{-}ol}$ fractionations that range from −0.01 to +0.21‰, and this fractionation is inversely correlated with the $\delta^{56}Fe$ values for the individual minerals (Fig. 3). Because of the inverse correlation between $\Delta^{56}Fe_{cpx\text{-}ol}$ and $\delta^{56}Fe$, it seems unlikely that the inter-mineral fractionations in these spinel peridotites are a result of equilibrium exchange of Fe isotopes at high temperature. Rather, we interpret the $\delta^{56}Fe_{clinopyroxene}$-$\delta^{56}Fe_{olivine}$ variations to reflect open-system processes, drawing on analogous relations that have been observed in oxygen isotope studies (e.g., Gregory and Criss, 1986). The $\Delta^{56}Fe_{cpx\text{-}ol}$ fractionations we observe correlate with mineral composition, where $\Delta^{56}Fe_{cpx\text{-}ol}$ fractionations are largest in cases where the most Fe-rich phase has the lowest $\delta^{56}Fe$ value (Fig. 4).

5.1. A Metasomatic Origin for Fe Isotope Variations in the Mantle

Considering the narrow range in Fe isotope compositions measured in igneous rocks ($\delta^{56}Fe = 0.00 \pm 0.05$‰; Beard et al., 2003a), we might expect that mantle rocks should also have a similarly narrow range. The relatively wide range in bulk-rock $\delta^{56}Fe$ values for the mantle-derived samples analyzed in this study, as well as that of Zhu et al. (2002), is therefore surprising. Although in most cases the bulk samples have $\delta^{56}Fe$ values near zero, that is not always the case, and in fact $\delta^{56}Fe$ values for bulk mantle samples vary from 0 to −0.5‰. Because the inter-mineral Fe isotope fractionations between olivine, orthopyroxene, and clinopyroxene do not appear to reflect equilibrium processes (above), the low $\delta^{56}Fe$ values measured in some of these mantle xenoliths are unlikely to have been produced by extraction of partial melts. Indeed, the most fertile samples (e.g., lowest forsterite content for olivine) have the lowest $\delta^{56}Fe$ values (Tables 2 and 4). We therefore interpret the anomalously low $\delta^{56}Fe$ values to reflect mantle metasomatism, which is a common process that produces mineralogic and/or elemental changes (Dawson, 1984; Nielson and Noller, 1987). Cryptic mantle metasomatism has been shown to affect the isotope compositions of O, Sr, Nd, and Pb in mantle minerals (Hauri et al., 1993; Zhang et al., 2000). Where ferrous and ferric contents of olivine, orthopyroxene, and clinopyroxene have been measured, it appears that neither patent nor cryptic metasomatic processes change the ferric to total Fe ratios, although the total Fe of the system may be increased (McGuire et al., 1991; Dyar et al., 1992).

If a metasomatic mechanism is the cause of the apparent disequilibrium Fe isotope fractionations between olivine and clinopyroxene in this suite of xenoliths, two endmember cases for the origin of Fe isotope variations in the mantle are possible. In the first case, we assume that the mantle has a homogenous Fe isotope composition equal to that measured in basaltic samples ($\delta^{56}Fe = 0.00 \pm 0.05$‰). In this case, the metasomatic fluid would be required to have a low $\delta^{56}Fe$ value to produce

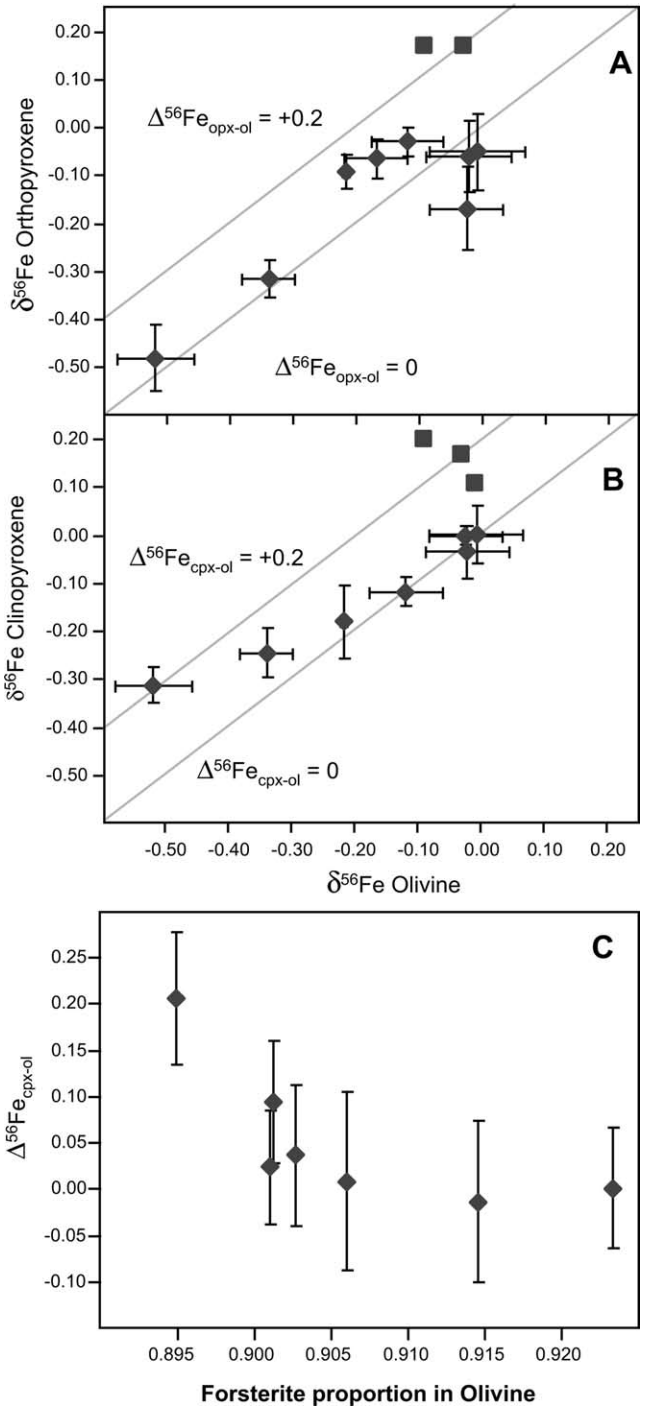

Fig. 3. Inter-mineral Fe isotope fractionations among olivine, orthopyroxene, and clinopyroxene in spinel peridotite mantle xenoliths. (A) Olivine-orthopyroxene fractionation. Error bars are the external 1 SD of the mean determined from two or more replicate analyses. Data are from this study (diamonds) and Zhu et al. (2002) (squares). There are no significant differences between the Fe isotope composition of olivine and orthopyroxene for the samples analyzed in this study, although the data of Zhu et al. (2002) appear to show a significant isotopic fractionation between olivine and orthopyroxene. (B) Olivine-clinopyroxene fractionations. The difference in the Fe isotope composition between clinopyroxene and olivine is larger as a function of their δ^{56}Fe values. (C) Plot of $\Delta^{56}Fe_{cpx-ol}$ vs. the forsterite content of olivine. $\Delta^{56}Fe_{cpx-ol}$ is largest for samples with the highest Mg content in olivine.

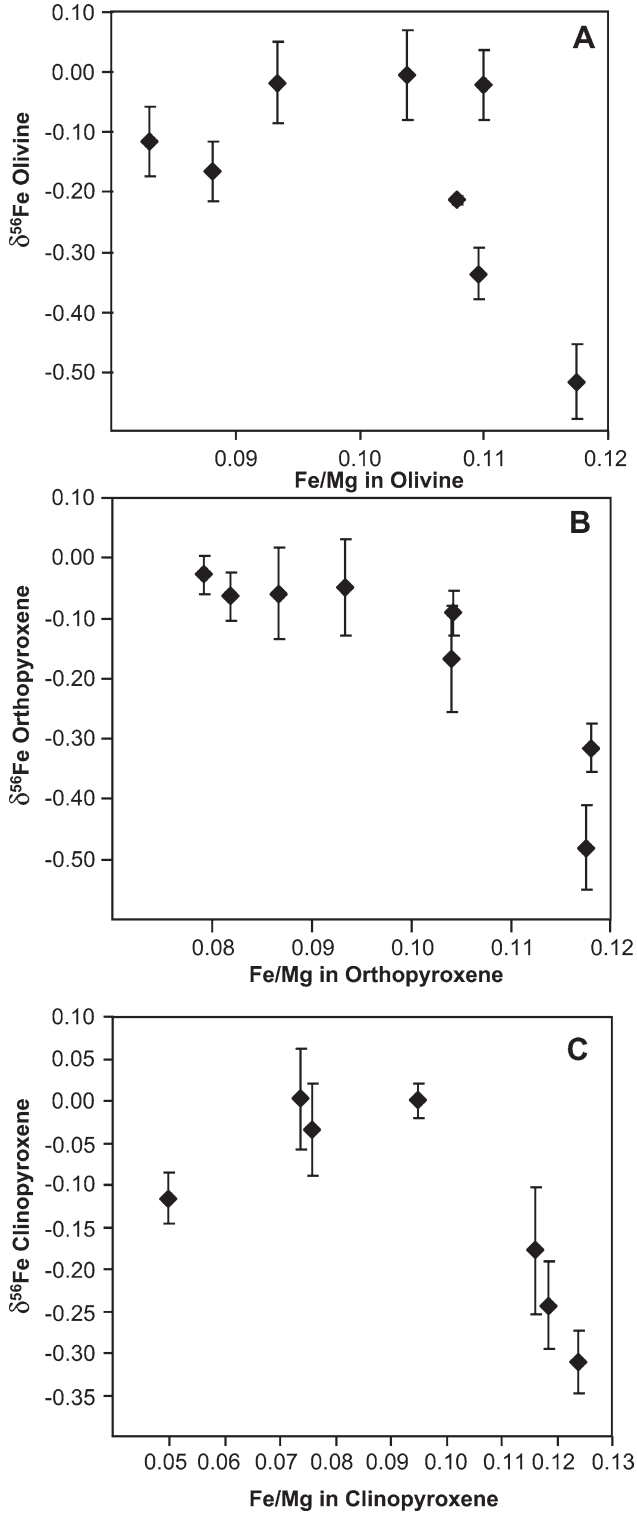

Fig. 4. Iron isotope compositions of olivine, orthopyroxene, and clinopyroxene as a function of Fe/Mg ratios of respective minerals. (A) δ^{56}Fe of olivine vs. Fe/Mg ratio. (B) δ^{56}Fe value of orthopyroxene vs. Fe/Mg ratio. (C) δ^{56}Fe value of clinopyroxene vs. Fe/Mg ratio. In general, the δ^{56}Fe value is lowest for samples with the highest Fe/Mg ratio, suggesting addition of a low-δ^{56}Fe, Fe-rich component, possibly through mantle metasomatism.

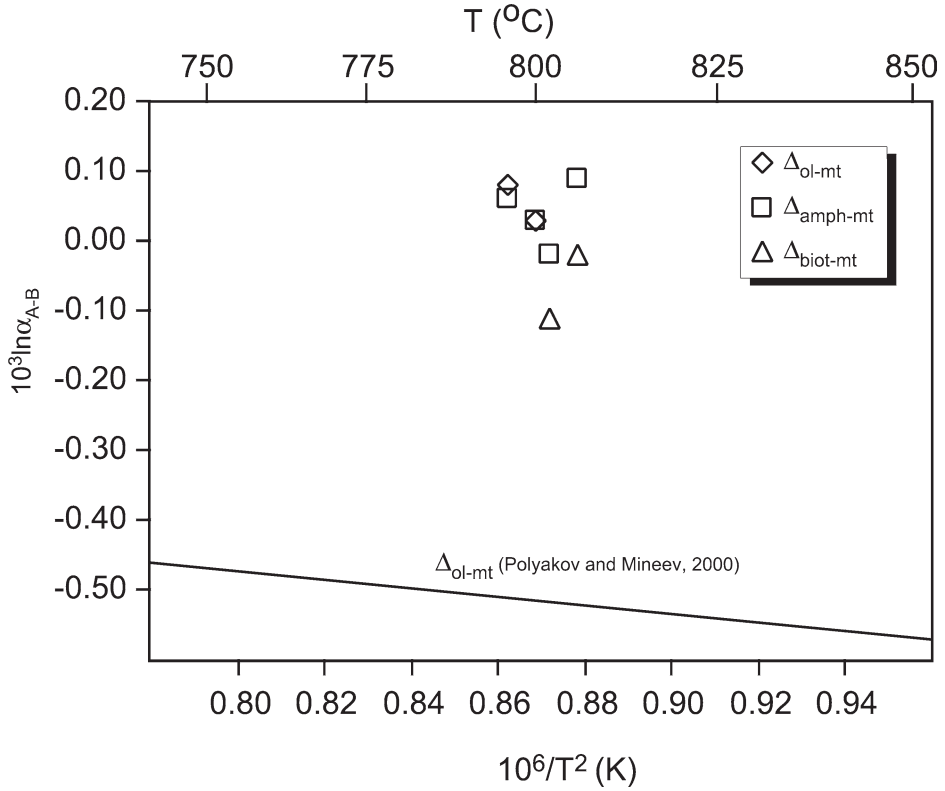

Fig. 5. $10^3 \ln\alpha_{A\text{-}B}$ fractionations for olivine-magnetite, amphibole-magnetite, and biotite-magnetite vs. the equilibration temperature of the rock determined by magnetite-ilmenite thermometry for four igneous rocks from the Chaos Crags, Mount Lassen, California. For comparison, the Fe isotope fractionation factor between olivine and magnetite calculated by Polyakov and Mineev (2000) based on spectroscopic data is shown.

the low δ^{56}Fe values measured in some of the xenoliths. The anomalous $\Delta^{56}Fe_{clinopyroxene\text{-}olivine}$ fractionations would therefore be interpreted to reflect more rapid Fe isotope equilibrium between olivine and fluid, relative to clinopyroxene, based on the fact that the δ^{56}Fe value for clinopyroxene is closer to that of the inferred initial value of zero. Relatively rapid Fe isotope exchange for olivine is consistent with Fe diffusion rates measured for olivine, orthopyroxene, and clinopyroxene (Ganguly and Tazzoli, 1994; Dimanov and Sautter, 2000; Gaetani and Watson, 2002). The origin of a mantle fluid that has a low δ^{56}Fe value is speculative, but some possibilities include Fe-bearing fluids derived from subducted sediments, CO_2-rich fluids, or carbonate metasomatic melts. Such fluids may be important agents in controlling chemical fluxes in the mantle (Hauri et al., 1993). The Fe isotope homogeneity of basaltic rocks would seem to rule out silicate melts as a metasomatic agent that could have low δ^{56}Fe values.

A second case presumes that the Fe isotope composition of the ambient mantle is variable. Although large portions of the mantle must be isotopically homogenous, based on the isotopic homogeneity of igneous rocks, it may be that only small parts of the mantle have low δ^{56}Fe values, that may be sampled as xenoliths through passage by, for example, alkalic basalts. In this case, the anomalous $\Delta^{56}Fe_{clinopyroxene\text{-}olivine}$ fractionations may be caused by interaction with a fluid that had a δ^{56}Fe value greater than that analyzed in the xenolith. This would require the high δ^{56}Fe values measured in some clinopyroxenes, relative to coexisting olivine, to preferentially reflect the fluid composition, which would require extensive Fe exchange in clinopyroxene relative to olivine; this conclusion, however, is at odds with Fe diffusion data (above). Relative diffusion rates notwithstanding, the relative Fe mass balance among mantle minerals supports this scenario, where the relatively low Fe contents of clinopyroxene would make this phase less resistant to changes in its δ^{56}Fe values as compared to olivine and orthopyroxene. In addition, the metasomatic agent in this scenario could easily be basaltic silicate melts because a fluid that had a δ^{56}Fe value of 0‰ is permissible in such a model.

5.2. Constraints on Fe Mass Transfer in the Earth

The range in δ^{56}Fe values for chondrite meteorites is similar to that of mantle-derived minerals (Beard and Johnson, 2004), which might suggest that the isotopic heterogeneity measured in mantle minerals is inherited from planetary accretion processes. Preservation of isotope heterogeneities from accretionary processes seems unlikely because there is no evidence for preservation of the O isotope anomalies that are common in chondritic meteorites (Clayton, 1993). Using the silicate-metal fractionations predicted by Polyakov and Mineev (2000), where, for example, fractionation between olivine and metal (α-Fe^O) is calculated to be +0.06 to +0.02‰ for $^{56}Fe/^{54}Fe$ ratios between 1000 and 2000°C, suggests that core formation is unlikely to impose isotopic heterogeneity on the mantle.

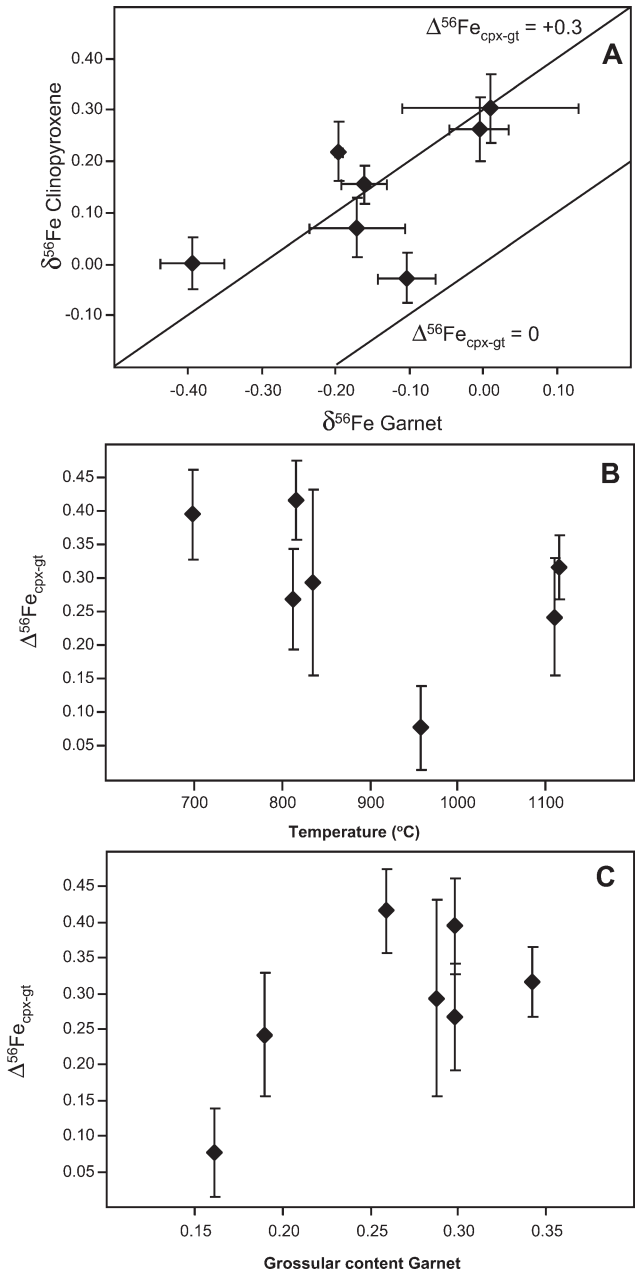

Fig. 6. Fe isotope fractionations, temperatures of equilibration, and chemical compositions of garnet in eclogites and ultramafic rocks. (A) δ^{56}Fe of garnet vs. that of coexisting clinopyroxene. Six of the seven samples scatter about a $\Delta^{56}Fe_{cpx-gt}$ of +0.3‰ over a wide range in δ^{56}Fe values measured in the minerals. Error bars are 1 SD of the mean as determined by two or more replicate analyses of the mineral. (B) $\Delta^{56}Fe_{cpx-gt}$ vs. the equilibration temperature of the rock calculated from Fe-Mg partitioning between garnet and clinopyroxene. Excluding sample CS-ND-3B, which has an anomalously low Ca concentration in garnet, samples with the largest garnet clinopyroxene fractionations have the lowest equilibration temperature. (C) $\Delta^{56}Fe_{cpx-gt}$ values vs. the grossular content in garnet. The sample with the smallest $\Delta^{56}Fe_{cpx-gt}$ values has the lowest grossularite content.

Mullane et al. (2002) report that silicate minerals from Pallasite minerals have a near-constant Fe isotope composition and that Fe metal in some Pallasites has a δ^{56}Fe value that is greater than coexisting silicate and in other Pallasites the metal has a δ^{56}Fe value that is less than coexisting silicate, supporting a small metal-silicate fractionation factor. Zhu et al. (2002), however, report a 0.2‰ fractionation between Fe-metal and coexisting olivine in Pallasite meteorites.

Although there may be some uncertainty regarding production of Fe isotope variations in the mantle due to accretion or core formation, we suggest that the data at hand indicate that mantle metasomatism is the most likely process to produce Fe isotope variability. Metasomatic activity may have been a result of fluids derived from subducted oceanic crust, by CO_2-rich fluids, or carbonatitic melts. Rouxel et al. (2003) have studied the Fe isotope composition of oceanic crust by analysis of bulk rocks from drill core of a Jurassic age segment of oceanic crust. Rouxel et al. (2003) measured δ^{56}Fe values between −1.8 and +1.3‰ for altered oceanic crust, where large variations in isotopic compositions are recorded in hydrothermal veins and zones in which Fe has been leached, as well as inter-pillow sediments. Although the range in δ^{56}Fe values in altered oceanic crust is relatively large, isotopic variability is apparently restricted to small scales, where the bulk δ^{56}Fe value for different sections of oceanic crust appears to be essentially identical to the bulk igneous values. Production of isotopically variable mantle through subduction of altered oceanic crust would therefore require selective removal of Fe from the crust, rather than simple bulk subduction. No data exist regarding the Fe isotope compositions of CO_2-rich fluids or carbonatitic melts.

Regardless of the origin of Fe isotope variability in the mantle, either through subduction of altered oceanic crust or intra-mantle differentiation and metasomatism, magma generation apparently homogenizes this isotopic variability (Fig. 7). Moreover, the lack of significant Fe isotope fractionation among the common Fe-bearing liquidus minerals in shallow magmas indicates that Fe isotope compositions will not change during magmatic differentiation at crustal pressures, consistent with the observation that the δ^{56}Fe values of rhyolites and granites are indistinguishable from those of basalts (Fig. 1; Beard et al., 2003a). The lack of significant Fe isotope variability in many clastic sedimentary rocks (Beard et al., 2003b) also limits the possibility of changes in δ^{56}Fe values of magmas though crustal interaction, which stands in contrast to, for example, oxygen isotope variations in igneous rocks (Eiler, 2001). We conclude that although there is apparently significant Fe isotope variability in the mantle, at least in the portions sampled by mantle xenoliths, the process of magma generation effectively isolates this variability to the mantle (Fig. 7). As a result, continental crust is largely homogeneous in its Fe isotope compositions, and significant Fe isotope variations only reappear in the Fe geochemical cycle in low-temperature aqueous environments (Fig. 7).

6. CONCLUSIONS

Coexisting olivine and clinopyroxene from some mantle-derived samples have distinct differences in Fe isotope composition, where the $\Delta^{56}Fe_{cpx-ol}$ fractionation increases with decreasing δ^{56}Fe values in olivine (or clinopyroxene). Moreover, minerals that have the lowest δ^{56}Fe values have the highest Fe contents and Fe/Mg ratios. These relations are interpreted to reflect isotopic disequilibrium produced by meta-

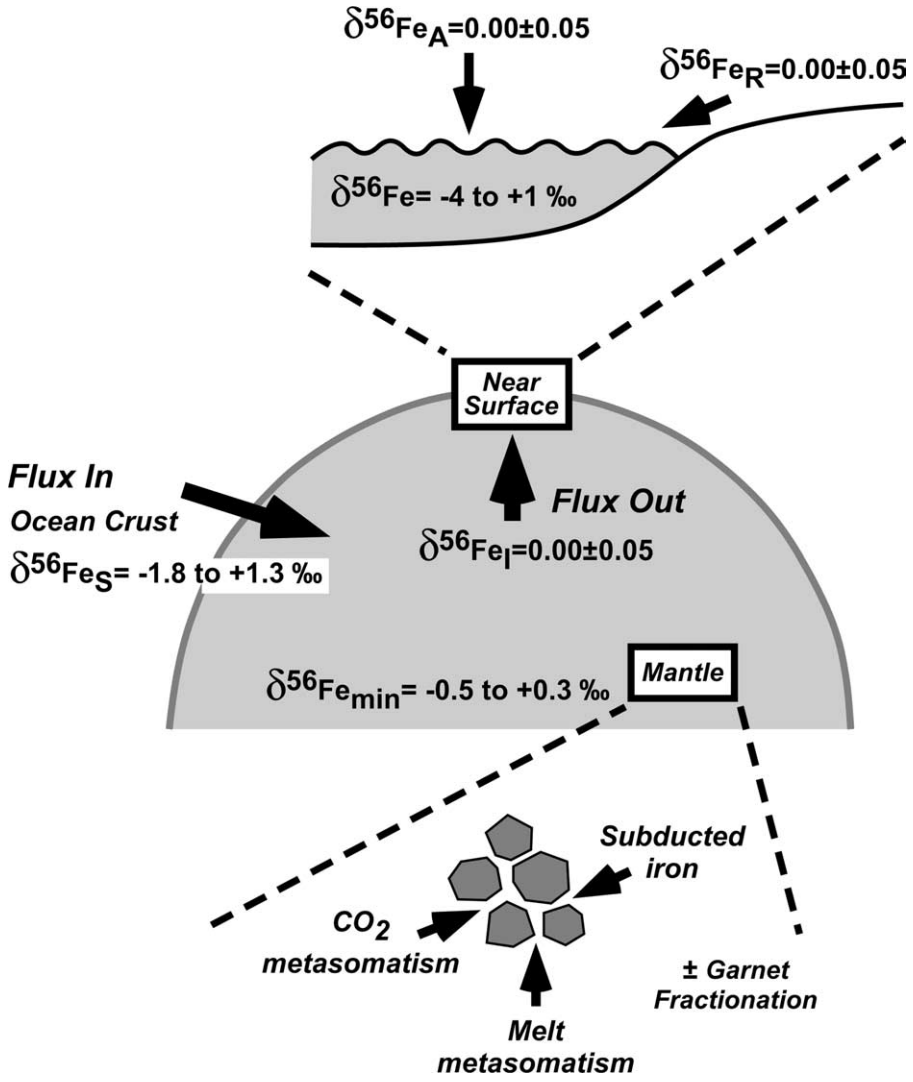

Fig. 7. Schematic representation of possible global Fe geochemical cycle. Subscripts for δ^{56}Fe values for various fluxes are: I = igneous rocks, S = subducted component, R = riverine suspended load, A = aerosol load. The flux of Fe out of the mantle in the form of igneous rocks has a constant δ^{56}Fe value of 0‰. In the near-surface environment this invariant Fe isotope composition is largely preserved in clastic sedimentary rocks. However, in environments where Fe undergoes redox changes, for example in anoxic basins where black shales are deposited or where dissimilatory iron-reducing bacteria are present, significant Fe isotope variations are produced (Johnson et al., 2002, 2003; Welch et al., 2003), as recorded in chemically precipitated sediments. Subduction processes return some of this anomalous Fe isotope composition material, and these anomalous compositions are transported through the mantle by metasomatic processes. The isotopic variability of the subducted component is based on analyses of oceanic crust from Rouxel et al. (2003).

somatic alteration in the mantle by fluids that have low δ^{56}Fe values. The differences in Fe isotope compositions between olivine and clinopyroxene, for example, may reflect the relatively rapid solid-state diffusion rates of Fe in olivine, and metasomatic addition of Fe. It is possible that the significant inter-mineral Fe isotope fractionations among olivine, orthopyroxene, and clinopyroxene reported by Zhu et al. (2002) for mantle xenoliths also reflect disequilibrium processes.

In contrast to the isotopic disequilibrium among minerals in some mantle xenoliths, there appears to be significant equilibrium Fe isotope fractionation between garnet and clinopyroxene. The average $\Delta^{56}Fe_{cpx\text{-}garnet}$ fractionation of six of the seven analyzed samples is $+0.32 \pm 0.07$‰. One sample, which has a low Ca content in garnet, has a low $\Delta^{56}Fe_{cpx\text{-}garnet}$ fractionation of 0.07‰. The inter-mineral Fe isotope differences in garnet and clinopyroxene appear to be produced by equilibrium Fe isotope exchange because there is little variation in $\Delta^{56}Fe_{cpx\text{-}garnet}$ fractionations over the range of δ^{56}Fe values. The range in δ^{56}Fe values measured in garnet and clinopyroxene is a function of the Fe mass balance of the samples. The bulk-rock eclogites and peridotites have δ^{56}Fe values near zero, similar to terrestrial igneous rocks, and therefore isotopic mass-balance of the mineral phases provides a check on the accuracy of the Fe isotope measurements. The δ^{56}Fe value of garnet from peridotite varies greatest because garnet is the minor Fe phase. In eclogites, clinopyroxene is generally the minor Fe

reservoir, and eclogitic clinopyroxenes have $\delta^{56}Fe$ values that are greater than those of igneous rocks.

There does not appear to be significant equilibrium inter-mineral fractionation between magnetite-olivine, -amphibole, or –biotite, in contrast, for example, to the calculated olivine-magnetite Fe isotope fractionations predicted by Polyakov and Mineev (2000), where they calculate that $\Delta^{56}Fe_{olivine\text{-}magnetite}$ should be $-0.5‰$ at 800°C. Moreover, our data do not corroborate the significant Fe isotope fractionations between magnetite and silicate minerals reported by Berger and von Blanckenburg (2001) although it is important to note that this discrepancy may in part be due to differences in temperatures and cooling history. There was no equilibrium fractionation of Fe isotopes between olivine and orthopyroxene in the spinel peridotites analyzed in this study, which agrees with $\Delta^{56}Fe_{opx\text{-}ol}$ calculated Fe isotope fractionation of $-0.03‰$ at 1000°C that is predicted by Polyakov and Mineev (2000). We do not observe, at least in our sample suite, the Fe isotope fractionations reported by Zhu et al. (2002) on spinel peridotites, where they measure $\Delta^{56}Fe_{opx\text{-}olivine}$ fractionations of $+0.20$ and $+0.26‰$ for two spinel peridotites.

The small, though significant Fe isotope variations recorded in the mantle-derived samples reported here and in Zhu et al. (2002) stand in contrast to the isotopic homogeneity of igneous rocks in oceanic and continental environments. The proportion of isotopically anomalous mantle must therefore be quite minor, and any contribution to basaltic melts must be small. Because there are no significant Fe isotope fractionations among the major Fe-bearing minerals (silicates and oxides) that are liquidus phases in magmas that differentiate at crustal depths, the isotopic homogeneity recorded in basaltic magmas will be retained during differentiation. The significant equilibrium clinopyroxene-garnet fractionation, however, suggests that crystal fractionation of basaltic magmas within the mantle may produce Fe isotope variations.

In terms of the global Fe cycle, the significant Fe isotope variability found in mantle minerals is apparently "left in the mantle" during magma genesis, and Fe isotope fractionations only reappear in natural systems in surface environments where low-temperature fractionations between fluids and minerals occur. It seems most likely that the origin of the variable Fe isotope composition in mantle minerals is ultimately tied to near-surface processes where the largest range in Fe isotope fractionations have been measured in natural samples. Return of variable Fe isotope compositions to the mantle most likely occurs through subduction processes.

Acknowledgments—We would like to thank Gordon Medaris and Garret Hart for supplying the well characterized garnet and magnetite bearing rocks used in this study. We also thank Howard Wilshire and Alan Glazner for help in collecting the western USA spinel peridotites. The Smithsonian Institute is thanked for allowing us access to Robert Coleman's Saudi Arabia xenolith collection. We thank John Fournelle for his expert help with the electron microprobe, and Brian Hess for preparing the mineral separate grain mounts. This work was supported by the NSF (EAR-0106614). We thank John Eiler, two anonymous reviewers, and Associate Editor Ed Ripley for their helpful comments.

Associate editor: E. Ripley

REFERENCES

Albarède F. and Beard B. L. (2004) Analytical methods for non-traditional stable isotopes. *Rev. Mineral. Geochem.* **55,** 113–152.

Beard B. L. and Johnson C. M. (2004) Fe isotope variations in the modern and ancient earth and other planetary bodies. *Rev. Mineral. Geochem.* **55,** 319–357.

Beard B. L., Medaris G. M. Jr., Johnson C. M., Brueckner H. K., and Mísa&rbreve;. (1992) Petrogenesis of Variscan high-temperature Group A eclogites from the Moldanubian zone of the Bohemian Massif. *Contrib. Mineral. Petrol.* **111,** 468–483.

Beard B. L., Johnson C. M., Skulan J. L., Nealson K. H., Cox L., and Sun H. (2003a) Application of Fe isotopes to tracing the geochemical and biological cycling of Fe. *Chem. Geol.* **195,** 87–117.

Beard B. L., Johnson C. M., von Damm K. L., and Poulson R. L. (2003b) Iron isotope constraints on Fe cycling and mass balance in oxygenated Earth oceans. *Geology* **31,** 629–632.

Berger A. and von Blanckenburg F. (2001) High-temperature fractionation of Fe isotopes. *Eos Trans AGU* **82,** abstr. V21A-0958.

Bradshaw A. M (2002) An electron microprobe study of Fe-Ti oxide minerals from Chaos Crags, Lassen volcanic center, California. Senior thesis, Department of Geology and Geophysics, University of Wisconsin-Madison, 35 pp.

Bussod G. Y. A. and Williams D. R. (1991) Thermal and kinematic model of the southern Rio Grande rift: Inferences from crustal and mantle xenoliths from Kilbourne Hole, New Mexico. *Tectonophysics* **197,** 373–389.

Chiba H., Chacko T., Clayton R. N., and Goldsmith J. R. (1989) Oxygen isotope fractionations involving diopside, forsterite, magnetite, and calcite: Application to geothermometry. *Geochim. Cosmochim. Acta* **53,** 2985–2995.

Clayton R. N. (1993) Oxygen isotopes in meteorites. *Ann. Rev. Earth Planet. Sci.* **21,** 115–149.

Dawson J. B. (1984) Contrasting types of upper-mantle metasomatism? In *Kinberlites II; The Mantle and Crust–Mantle Relationships* (ed. J. Kornprobst), pp. 289–294. Elsevier, Amsterdam.

Dimanov A. and Sautter V. (2000) "Average" interdiffusion of (Fe,Mn)-Mg in natural diopside. *Eur. J. Mineral.* **12,** 749–760.

Dyar M. D., McGuire A. V., and Harrell M. D. (1992) Crystal chemistry of iron in two styles of metasomatism in the upper mantle. *Geochim. Cosmochim. Acta* **56,** 2579–2586.

Eiler J. M. (2001) Oxygen isotope variations of basaltic lavas and upper mantle rocks. In *Stable Isotope Geochemistry, Reviews of Mineralogy and Geochemistry*, Vol. 43 (eds. J. W. Valley and D. R. Cole), pp. 319–364. Mineralogical Society of America.

Ellis D. J. and Green D. H. (1979) An experimental study of the effect of Ca upon garnet-clinopyroxene Fe-Mg exchange equilibria. *Contrib. Mineral. Petrol.* **71,** 13–22.

Ernst W. G. (1977) Mineralogic study of eclogitic rocks from Alpe Arami, Lepontine Alps, southern Switzerland. *J. Petrol.* **18,** 371–398.

Gaetani G. A. and Watson E. B. (2002) Modeling the major-element evolution of olivine-hosted melt inclusions. *Chem. Geol.* **183,** 25–41.

Ganguly J. and Tazzoli V. (1994) Fe^{2+}-Mg interdiffusion in orthopyroxene: Retrieval from the data on intracrystalline exchange reaction. *Am. Min.* **79,** 930–937.

Gregory R. T. and Criss R. E. (1986) Isotopic exchange in open and closed systems. In *Stable Isotopes in High Temperature Geological Processes* (eds. J. W. Valley, H. P. Taylor Jr., and J. R. O'Neil), pp. 91–128. *Reviews in Mineralogy*, Vol. 16, Mineralogical Society of America, Washington, DC.

Hauri E. H., Shimizu N., Dieu J. J., and Hart S. R. (1993) Evidence for hotspot-related carbonatite metasomatism in the oceanic upper mantle. *Nature* **365,** 221–227.

Heiken G. and Eichelberger J. C. (1980) Eruptions at Chaos Crags, Lassen Volcanic National Park, California. *J. Volcan. Geohterm. Res.* **7,** 443–481.

Johnson C. M., Skulan J. L., Beard B. L., Sun H., Nealson K. H., and Braterman P. S. (2002) Isotopic fractionation between Fe(III) and Fe(II) in aqueous solutions. *Earth Planet. Sci. Lett.* **195,** 141–153.

Johnson C. M., Beard B. L., Beukes N. J., Klein C., and O'Leary J. M. (2003) Ancient geochemical cycling in the Earth as inferred from Fe isotope studies of banded iron formations from the Transvaal Craton. *Contrib. Mineral. Petrol.* **144,** 523–547.

Kohn M. J. and Valley J. W. (1998) Effects of cation substitutions in

garnet and pyroxene on equilibrium oxygen isotope fractionations. *J. Metamorphic Geol.* **16,** 625–639.

McGuire A. V. (1988) The mantle beneath the Red Sea margin: Xenoliths from western Saudi Arabia. *Tectonophysics* **150,** 101–119.

McGuire A. V. and Bohannon R. G. (1989) Timing of mantle upwelling: Evidence for a passive origin for the Red Sea Rift. *J. Geophys. Res.* **94,** 1677–1682.

McGuire A. V., Dyar M. D., and Nielson J. E. (1991) Metasomatic oxidation of upper mantle peridotite. *Contrib. Mineral. Petrol.* **109,** 252–264.

Medaris L. G. Jr., Wang H. F., Mísǎr Z., and Jelínek E. (1990) Thermobarometry, diffusion modeling and cooling rates of crustal garnet peridotites: Two examples from the Moldanubian Zone of the Bohemian Massif. *Lithos.* **25,** 189–202.

Medaris L. G. Jr., Beard B. L., Johnson C. M., Valley J. W., Spicuzza M. J., Jelínek E., and Mísǎr Z. (1995a) Garnet pyroxenite and eclogite in the Bohemian Massif: Geochemical evidence for the Variscan recycling of subducted lithosphere. *Geol. Rundsch.* **84,** 489–505.

Medaris L. G. Jr., Jelínek E., and Mísǎr Z. (1995b) Czech eclogites. Terrane settings and implications for Variscan tectonic evolution of the Bohemian Massif. *Eur. J. Min.* **7,** 7–28.

Mullane E., Russel S. S., and Gounelle M. (2002) Iron isotope fractionation within a differentiated asteroidial sample suite. 65th Ann. Meteoritical Society Meeting, abstr. 5157.

Neville S. L., Schiffman P., and Sadler P. M. (1983) New discoveries of spinel lherzolite and garnet websterite nodules in alkaline basalts from the south-central Mojave Desert and northeast Transverse Ranges, California. *Geol. Soc. Am. Abst. Prog.* **15,** 302.

Nielson J. E, Noller J. S (1987) Processes of mantle metasomatism; Constraints from observations of composite xenoliths. In *Mantle Metasomatism and Alkaline Magmatism* (eds. E. M. Morris and J. D. Pasteris), pp. 61–76. Geol. Soc. Am. Spec. Paper 215.

Polyakov V. B. and Mineev S. D. (2000) The use of Mössbauer spectroscopy in stable isotope geochemistry. *Geochim. Cosmochim. Acta* **64,** 849–865.

Rouxel O., Bobbek N., Ludden J., and Fouquet Y. (2003) Iron isotope fractionation during oceanic crust alteration. *Chem. Geol.* **202,** 155–182.

Skulan J. L., Beard B. L., and Johnson C. M. (2002) Kinetic and equilibrium Fe isotope fractionation between aqueous Fe(III) and hematite. *Geochim. Cosmochim. Acta* **66,** 2995–3015.

Taylor H. P. Jr. and Sheppard S. M. F. (1986) Igneous rocks: I. Processes of isotopic fractionation and isotope systematics. In *Stable Isotopes in High Temperature Geological Processes* (eds. J. W. Valley, H. P. Taylor Jr., and J. R. O'Neil), pp. 227–271. *Reviews in Mineralogy*, Vol. 16. Mineralogical Society of America, Washington, DC.

Taylor P. D. P., Maeck R., and De Bièvre P. (1992) Determination of the absolute isotopic composition and atomic weight of a reference sample of natural iron. *Int. J. Mass Spectrom. Ion Processes* **121,** 111–125.

Taylor P. D. P., Maeck R., Hendrickx F., and De Bièvre P. (1993) The gravimetric preparation of synthetic mixtures of iron isotopes. *Int. J. Mass Spectrom. Ion Processes* **128,** 91–97.

Taylor W. R. (1998) An experimental test of some geothermometer and geobarometer formulations for upper mantle peridotites with application to the thermobarometry of fertile lherzolite and garnet websterite. *N. Jb. Miner. Abh.* **172,** 381–408.

Valley J. W., Bindeman I. N., and Peck W. H. (2003) Empirical calibration of oxygen isotope fractionation in zircon. *Geochim. Cosmochim. Acta* **67,** 3257–3266.

Welch S. A., Beard B. L., Johnson C. M., and Braterman P. S. (2003) Kinetic and equilibrium Fe isotope fractionation between aqueous Fe(II) and Fe(III). *Geochim. Cosmochim. Acta* **67,** 4231–4250.

Wilshire H. G., Meyer C. E., Nakata J. K., Calk L. C., Shervais J. W., Nielson J. E., and Schwarzman E. C. (1988) Mafic and ultramafic xenoliths from volcanic rocks of the western United States. *U.S. Geol. Surv. Prof. Paper* **1443,** 179 pp.

Zhang D. P., Mattey D. P., Grassineau N., Lowry D., Brownless M., Gurney J. J., and Menzies M. A. (2000) Recent fluid processes in the Kaapvaal Craton, South Africa: Coupled oxygen isotope and trace element disequilibrium in polymict peridotites. *Earth Planet. Sci. Lett.* **176,** 57–72.

Zhu X. K., Guo Y., Williams R. J. P., O'Nions R. K., Matthews A., Belshaw N. S., Canters G. W., de Waal E. C., Weser U., Burgess B. K., and Salvato B. (2002) Mass fractionation processes of transition metal isotopes. *Earth Planet. Sci. Lett.* **200,** 47–62.